行政院國家科學委員會專題研究計畫 成果報告

小鼠染色體 14A3 區性腺表現基因群的分子特性與功能分析 (第 3 年)
研究成果報告(完整版)

計 畫 類 別 ：個別型
計 畫 編 號 ：NSC 97-2320-B-040-010-MY3
執 行 期 間 ：99 年 08 月 01 日至 100 年 07 月 31 日
執 行 單 位 ：中山醫學大學生物醫學科學學系（所）

計 畫 主 持 人：王淑紅

計畫參與人員：碩士班研究生-兼任助理人員：黃瑞喜
碩士班研究生-兼任助理人員：黃士玲
大專生-兼任助理人員：李國智
大專生-兼任助理人員：邱瓊儀
大專生-兼任助理人員：吳源逸
大專生-兼任助理人員：王忻慈
大專生-兼任助理人員：李忠融

公 開 資 訊 ：本計畫涉及專利或其他智慧財產權，2 年後可公開查詢

中 華 民 國 100 年 11 月 01 日

中文摘要：　此計畫的最終目的是想了解在哺乳動物中，生殖細胞生成及早期胚胎發育之整個遺傳機制。本計畫研究 14A3 區已知母源性基因 Cphx 及下游之 Duxbl 及 Gcse 基因的功能，首先根據我們已發表研究顯示 Cphx gene 是一個大量表現在卵細胞中的同源箱基因，同時也是一個母源性的基因，我們產製 Cphx-dsRNA 基因轉殖鼠，以 RNAi 方式抑制 Cphx 基因表現，發現轉殖基因套數較多之 M50D 轉殖鼠，有明顯的生育能力下降的狀況，卵巢組織中之卵細胞數目比衛兵鼠減少 16%，而且基因轉殖鼠明顯有提早不孕的現象，不孕之基因轉殖鼠其卵巢濾泡數目減少同時卵巢形狀也異常，我們也發現沒有 TG/TG 轉殖小鼠的存在，以 Cphx-dsRNA 打入 GV oocyte 及受精卵都明顯的抑制卵細胞的成熟與早期胚胎的發育，因此我們推論 Cphx 在卵細胞發育成熟與早期胚胎發育扮演重要角色。位於 Cphx 下游之 Duxbl gene 屬於雙同源箱基因(double homeobox gene)，與造成人類顏面及肩胛肱肌肉失養症(FSHD)之候選基因 DUX4 同源箱區的相似度最高，因此對於小鼠 Duxbl 基因的研究將有助於我們對人類顏面及肩胛肱肌肉失養症致病機制的了解。由我們已發表的結果顯示，胚胎發育過程中 Duxbl 參與體腔及四肢肌肉的發育過程，Duxbl 基因表現在骨骼肌中之肌管細胞，但出生後小鼠的肌纖維組織中，Duxbl 表現明顯的降低，成熟肌肉組織中幾乎測不到 Duxbl 基因的表現，由於正常人類成熟肌肉組織也沒有 DUX4 基因的表現，因此我們推測可能是應該在胚胎時期表現的 DUX4 蛋白異常的表現於成熟組織因而造成 FSHD 疾病的生成。除了體腔骨骼肌外，我們發現眼外肌甚至眼球組織及生殖細胞也有 Duxbl 基因的表現，顯示 Duxbl 基因對於眼球的發育及生殖細胞的發育也扮演重要的角色。另外位於 Duxbl 基因下游的 Gcse 基因是一個新穎的生殖細胞特異性表達的基因，Gcse 轉錄出兩種主要的 mRNA: Gcse-l 與 Gcse-s，Gcse-l 與 Gcse-s 蛋白的 N 端 118 個氨基酸組成一致，而 Gcse-s 蛋白的 C 端有 56 個胺基酸與人類 AKT2（Protein kinase B）的催化區域高達 50%的相似度。從 Northern blots、 RT-PCR、原位雜交與組織化學免疫染色分析實驗發現，Gcse-l 專一表現於卵細胞，從進入減數分裂的卵母細胞到成熟卵細胞皆有 Gcse-l 表現，然而在受精卵中並未偵測到 Gcse-l mRNA 的表現。在睪丸組織中 Gcse-l 蛋白存在於精母細胞核內，而在減數分裂完成的單倍體精細胞及副睪之成熟精細胞中，則發現 Gcse-l 蛋白會轉移頂體構造，與頂體標記蛋白－Lectin-PNA 訊號位置重疊，而 Gcse-s 只在早期的單倍體圓精細胞偵測到訊號，根據 Gcse 在生殖細胞的表現分佈我們推測 Gcse 與生殖細胞的形成有關。

英文摘要：　The specific goal of this research proposal is to determine the developmental functions of Cphx, Duxbl and Gcse, in mouse

chromosome 14A3. Cphx gene is a maternal homeobox gene specifically expressed in oocytes. We produce Cphx-dsRNA transgenic mice to investigate the function of Cphx involve in oogenesis and early embryo development. The reproduction ability of high copy number Cphx-dsRNA transgenic mice was decreased and become infertile at about 8 month. In addition, oocyte maturation and early embryo development was inhibited by direct microinjection of Cphx dsRNA in germinal vesicle oocytes and 2 pronucleus embryos. We suggest that Cphx paly a role in oogenesis and early embryo development. On the other hand, the amino acid sequences of homeodomains in double homeobox gene Duxbl are most similar to those of human DUX4 protein, associated with facioscapulohumeral muscular dystrophy (FSHD). During embryonic development, Duxbl proteins were detected in trunk, limb and extraocular muscle and in elongated myocytes and myotubes. In adult tissues, Duxbl is predominantly expressed in female reproductive organs and eyes, and slightly expressed in brain and testes. We suggest that Duxbl proteins play regulatory roles during myogenesis, reproductive and eye development. The third gene, Gcse produce two transcripts: Gcse-l and Gcse-s in length. Gcse-l specifically expressed in both male and female germ cells, but Gcse-s expressed in male germ cell only. During spermatogenesis, strong Gcse-l transcripts were detected in late pachytene spermatocytes and round spermatids. However, Gcse-s transcripts were only existed in round spermatids. Gcse-l were detected in the nucleus of late pachytene spermatocytes. During meiosis, Gcse-l was translocated to acrosome region of spermatid and maintain in acrosome of spermatozoa. However, Gcse-s proteins expressed in cell nucleus of spermatid. We suggest that Gcse-l paly a role in oogenesis and spermatogenesis.

中、英文摘要及關鍵詞 (keywords)

(一).中文摘要:

此計畫的最終目的是想了解在哺乳動物中,生殖細胞生成及早期胚胎發育之整個遺傳機制。本計畫研究 14A3 區已知母源性基因 *Cphx* 及下游之 *Duxbl* 及 *Gcse* 基因的功能，首先根據我們已發表研究顯示 *Cphx* gene 是一個大量表現在卵細胞中的同源箱基因，同時也是一個母源性的基因，我們產製 Cphx-dsRNA 基因轉殖鼠，以 RNAi 方式抑制 *Cphx* 基因表現，發現轉殖基因套數較多之 M50D 轉殖鼠，有明顯的生育能力下降的狀況，卵巢組織中之卵細胞數目比衛兵鼠減少 16%，而且基因轉殖鼠明顯有提早不孕的現象，不孕之基因轉殖鼠其卵巢濾泡數目減少同時卵巢形狀也異常，我們也發現沒有 TG/TG 轉殖小鼠的存在，以 Cphx-dsRNA 打入 GV oocyte 及受精卵都明顯的抑制卵細胞的成熟與早期胚胎的發育，因此我們推論 *Cphx* 在卵細胞發育成熟與早期胚胎發育扮演重要角色。位於 *Cphx* 下游之 *Duxbl* gene 屬於雙同源箱基因(double homeobox gene)，與造成人類顏面及肩胛肱肌肉失養症(FSHD)之候選基因 DUX4 同源箱區的相似度最高，因此對於小鼠 *Duxbl* 基因的研究將有助於我們對人類顏面及肩胛肱肌肉失養症致病機制的了解。由我們已發表的結果顯示，胚胎發育過程中 *Duxbl* 參與體腔及四肢肌肉的發育過程，*Duxbl* 基因表現在骨骼肌中之肌管細胞，但出生後小鼠的肌纖維組織中，*Duxbl* 表現明顯的降低，成熟肌肉組織中幾乎測不到 *Duxbl* 基因的表現，由於正常人類成熟肌肉組織也沒有 *DUX4* 基因的表現，因此我們推測可能是應該在胚胎時期表現的 DUX4 蛋白異常的表現於成熟組織因而造成 FSHD 疾病的生成。除了體腔骨骼肌外，我們發現眼外肌甚至眼球組織及生殖細胞也有 *Duxbl* 基因的表現,顯示 *Duxbl* 基因對於眼球的發育及生殖細胞的發育也扮演重要的角色。另外位於 *Duxbl* 基因下游的 *Gcse* 基因是一個新穎的生殖細胞特異性表達的基因,Gcse 轉錄出兩種主要的 mRNA: *Gcse-1* 與 *Gcse-s*,Gcse-1 與 Gcse-s 蛋白的 N 端 118 個氨基酸組成一致，而 Gcse-s 蛋白的 C 端有 56 個胺基酸與人類 AKT2 (Protein kinase B)的催化區域高達 50%的相似度。從 Northern blots、RT-PCR、原位雜交與組織化學免疫染色分析實驗發現，*Gcse-1* 專一表現於卵細胞，從進入減數分裂的卵母細胞到成熟卵細胞皆有 *Gcse-1* 表現，然而在受精卵中並未偵測到 *Gcse-1* mRNA 的表現。在睪丸組織中 Gcse-1 蛋白存在於精母細胞核內,而在減數分裂完成的單倍體精細胞及副睪之成熟精細胞中，則發現 Gcse-1 蛋白會轉移頂體構造，與頂體標記蛋白－Lectin-PNA 訊號位置重疊，而 *Gcse-s* 只在早期的單倍體圓精細胞偵測到訊號，根據 *Gcse* 在生殖細胞的表現分佈我們推測 *Gcse* 與生殖細胞的形成有關。

關鍵字:卵細胞生成，精細胞生成，肌肉發育，同源箱基因，生殖細胞專一性表達基因，雙同源箱基因，人類顏面及肩胛肱肌肉失養症，頂體形成，同源箱區，Cphx, Duxbl, Gcse, DUX4

(二).英文摘要

The specific goal of this research proposal is to determine the developmental functions of *Cphx*, *Duxbl* and *Gcse*, in mouse chromosome 14A3. *Cphx* gene is a maternal homeobox gene specifically expressed in oocytes. We produce Cphx-dsRNA transgenic mice to investigate the function of *Cphx* involve in oogenesis and early embryo development. The reproduction ability of high copy number *Cphx*-dsRNA transgenic mice was decreased and become infertile at about 8 month. In addition, oocyte maturation and early embryo development was inhibited by direct microinjection of Cphx dsRNA in germinal vesicle oocytes and 2 pronucleus embryos. We suggest that *Cphx* paly a role in oogenesis and early embryo development. On the other hand, the amino acid sequences of homeodomains in double homeobox gene Duxbl are most similar to those of human DUX4 protein, associated with facioscapulohumeral muscular dystrophy (FSHD). During embryonic development, Duxbl proteins were detected in trunk, limb and extraocular muscle and in elongated myocytes and myotubes. In adult tissues, *Duxbl* is predominantly expressed in female reproductive organs and eyes, and slightly expressed in brain and testes. We suggest that Duxbl proteins play regulatory roles during myogenesis, reproductive and eye development. The third gene, *Gcse* produce two transcripts: *Gcse-l* and *Gcse-s* in length. *Gcse-l* specifically expressed in both male and female germ cells, but *Gcse-s* expressed in male germ cell only. During spermatogenesis, strong *Gcse-l* transcripts were detected in late pachytene spermatocytes and round spermatids. However, *Gcse-s* transcripts were only existed in round spermatids. Gcse-l were detected in the nucleus of late pachytene spermatocytes. During meiosis, Gcse-l was translocated to acrosome region of spermatid and maintain in acrosome of spermatozoa. However, Gcse-s proteins expressed in cell nucleus of spermatid. We suggest that Gcse-l paly a role in oogenesis and spermatogenesis.

Key words: oogenesis, spermatogenesis, early embryo development, homeobox gene, myogenesis, germ cell specific expressed gene, FSHD, double homeobox gene, homeodomain, acrosome formation, *Cphx*, *Duxbl*, *Gcse*,*DUX4*

前言、

本研究計畫延續過去研究之 14A3 區 *Cphx*, *Duxbl* 及 *Gcse* 基因群之研究，其中 *Cphx* 屬於卵細胞專一表達基因，*Duxbl* 雖然參與胚胎時期肌肉細胞的發育，但也可以在精原幹細胞及卵細胞中表現，而 *Gcse* 基因則是專一性表達於生殖細胞，其中 *Cphx* 及 *Duxbl* 皆屬於同源箱基因，同時在染色體上分別有兩個及三個重複序列。同源箱基因家族（homeobox gene families）是一群轉錄調節因子的基因群組，其蛋白產物可藉由調節下游基因的表現，而調控生物個體之發育過程（De Rebertis, E.M., 1994），除了可以影響胚胎時期動物之發育，掌控細胞分化及引導器官之形成。在年幼動物體的第二性徵之產生中，同源箱基因也佔有重要的調控角色（Gehring, et al., 1994）。此群基因最早由果蠅中發現，當同源箱基因 Antennapedia(Antp)發生突變，會產生果蠅觸角異位現象(McGinnis, et al., 1984)。往後的研究發現參與果蠅發育之基因都含有一段高度保留之序列，稱為同源箱（homeobox），故命名之。此段高度保留區可轉譯出約 60 個胺基酸，形成 helix-turn-helix 的結構，其中第三個螺旋會辨識特定的 DNA 序列與之結合因而調節基因之表現（Gehring, et al., 1994）。根據其高度保留之核酸序列的特徵，脊椎動物之同源箱基因可以分成不同家族，目前已有一群生殖相關的同源箱基因群 *Rhox*（reproductive homeobox gene)被發現(MacLean et al., 2005)，*Rhox* 基因群位於位於 X 染色體上的 A2 區，與我們正在研究的 14A3 區的基因一樣都位於染色體的端點上，Rhox 基因群會選擇性的表達在雄性及雌性生殖組織，根據基因群在染色體上的前後位置不同，其表現的時間點也會有互相銜接的現象，同時基因群中不同的基因也都有不同的細胞專一性的表現，這些基因群有些也具有功能上的重複性，當其中一個基因缺失時另外的基因可以取代它的功能，目前我們研究的 14A3 區的基因: *Cphx*, *Duxbl* 及 *Gcse* 同樣的以基因群的方式選擇性的表達在雄性及雌性生殖細胞，14A3 區除了我們已發表且正在研究中的 *Cphx* 及 *Duxbl* 同源箱基因分別帶有兩個及三個重覆序列之外，其中的 *Plac9* 基因也帶有兩個重覆序列(Galaviz-Hernandez et al., 2003)，*Gcse* 只有一個重覆序列，*Cphx* 專一的表現於卵細胞，而下游的 *Duxbl* 則會表現於卵細胞及精原細胞，*Gcse* 也表現於卵細胞，及進入減數分裂的精細胞，三個基因都在卵細胞發育的過程會表現，但在精細胞發育的過程，*Duxbl* 與 *Gcse* 的表現也呈現接力的現象，此種以基因群的方式共同調控生殖系統的方式，對於生殖能力強的嚙齒動物而言可能具有演化上的優勢；或者在基因群周圍可能存在著一些特異性的調控序列，負責此複雜又精密的調控，其詳細機制並不清楚。

研究目的、

本研究計畫將探討 14A3 區 *Cphx, Duxbl* 及 *Gcse* 基因群對於生殖系統與早期胚胎發育所扮演的角色，將分別了解此三個基因的功能及其之間是否有如 *Rhox* 基因群一樣，共同以時間與空間的結合方式影響生殖系統的發育。目前對於生殖系統與早期胚胎發育之分子機制未知的比已知的多，尤其是人類，主要受限於道德法律的規範問題，而老鼠卻提供了一個很好的動物模式，來研究早期胚胎發育的分子機制。即便如此，根據 cDNA library 及 EST database 的分析結果發現，在早期胚胎發育中表現的基因大部分是未知功能的基因。為了發掘參與早期胚胎發育之未知功能同源箱基因(Wang et al., 2003)，我們根據同源箱區中之高度保留的氨基酸序列，設計退化寡核酸引子，進行 PCR 反應篩選小鼠胚胎幹細胞 cDNA 基因庫，發現一些新的同源箱基因，包括已發表 *ENK(Nanog)*(Wang et al.,2003), *Cphx*(Li et al., 2006a)及已發表的 *Duxbl*(Wu et al., 2010)基因，這些同源箱基因同時表現在胚胎幹細胞及卵巢組織中之卵細胞或睪丸組織中的精細胞中，由於生殖細胞的發育成熟是一個相當複雜的過程，目前對於調控的分子機制所知有限。因此，研究 14A3 區生殖細胞表現基因群之功能將有助於了解生殖細胞成熟發育及早期胚胎之發育機制，對於目前不孕症的發生與診斷治療有一定程度的幫助。

文獻探討、

(一). *Cphx* gene

本研究計畫中的 *Cphx* 同源箱基因屬於卵細胞專一性表達的同源箱基因，過去的研究指出卵細胞專一性表達的同源箱基因 *Nobox* 的缺失造成小鼠不孕 Rajkovic et al., 2004)，最近的研究顯示有些卵巢提早退化的病人(premature ovarian failure; POF)，其 *Nobox* 基因產生同源箱區的突變進而影響其與下游基因結合的能力，因此 *Nobox* 基因的突變對一些 POF 病人而言可能是致病因素之一 (Qin et al.,2007)，顯示同源箱基因在卵細胞發育上確實扮演重要的角色。除了同源箱基因外，已知調節卵細胞基因表現的轉錄因子，如 *Figla* (Factor In the GermLine, Alpha)對於生殖也扮演很重要的角色 (Liang et al., 1997; Soyal et al., 2000)， *Figla* 基因踢除母鼠其胚胎時期性腺發育正常，但出生後卵巢組織無法形成 primordial follicle，同時卵細胞在數天之內消失，顯示 *Figla* 對於生殖細胞及 follicle 的發育扮演很重要的角色，由最近 *Figla* 基因踢除母鼠卵巢 microarray 的分析(Joshi et al., 2006)，發現本研究計畫中的 *Cphx* 表現也下降了，表示 *Figla* 蛋白直接或間接的調控 *Cphx* 基因的表現，因而影響卵細胞的成熟發育。本研究計畫以直接受 *Figla* 蛋白調控的 *Zp3* 基因的 promoter 啟動 Cphx-dsRNAi 的表現，分析 *Cphx* 表現下降對卵細胞成熟或早期胚胎發育的影響。

(二) *Duxbl*:

本研究計畫中的 *Duxbl* 基因屬於雙同源箱基因家族(DUX)，過去的研究顯示，DUX 只存在於人類與靈長類中，嚙齒類生物並不存在，同時 DUX 基因是沒有 intron 的，人類 *DUX* 基因通常會出現在染色體的重複片段中，其中，位於四號染色體 D4Z4 區的重複片段若有缺失，則可能會造成顏面及肩胛肱肌肉失養症 (FSHD:Facioscapulohumeral Muscular Dystrophy)，FSHD 是第三種常見的遺傳性的肌肉萎縮症。雖然人類 *DUX* 基因家族已經被發現很久，也有不同的 *DUX* 基因存在，但由於在正常組織中沒有 *DUX* 基因的表現，目前也只有 DUX1 及 DUX4 蛋白被證實存在於 FSHD 病人的肌肉母細胞萃取物中，對於 DUX 蛋白的正常生理功能，及其兩個同源箱區的各別特性及功能都還不是很了解，兩個同源箱區是否各自有結合 DNA 的能力，並調控不同基因的表現？又會調節哪些下游基因？都尚待研究。小鼠 *Duxbl* 基因除了是嚙齒類第一個 Dux 基因之外，已知的 DUX 基因組成並不含 intron，但 *Duxbl* 基因除了有 intron 之外，還包含不同的 splicing form。分析小鼠 *Duxbl* 基因在染色體上的分佈，發現也有三個 tandom repeat 的現象，同時位於 *Cphx* 基因的下游，*Duxbl* 也主要表現於卵巢組織及胚胎時期的睪丸組織，因此對 *Duxbl* 基因的確認與功能分析，將直接或間接有助於我們對卵巢或睪丸組織的發育或 FSHD 疾病的了解。

(三).*Gcse* gene

根據 Unigene database 及定量 PCR 的分析，發現小鼠基因體 4%的基因只表現於單倍體雄性生殖細胞中(Shultz, et al., 2003)，進一步分離 spermatocyte 或 round spermatid 並分析其基因表現，發現其中分別有 11%或 22%的基因屬於睪丸專一性的，而這些睪丸專一性的基因，有一半以上其功能未知(Hong et al., 2005; Choi et al., 2007)，因此研究精細胞專一表達基因，將有助於我們瞭解不孕症雄性患者之雄性生殖細胞發育的缺失，對於發展避孕藥也有幫助，由於破壞精細胞專一表達基因尤其是表現於精子發生期（Spermiogenic phase）的基因，對體細胞及 spermatogonia 較少副作用。本研究中之 *Gcse* 基因除了表現於卵細胞外，也專一性的表現於雄性生殖細胞，進入減數分裂的 spermatocyte 開始有 Gcse 蛋白的表現，減數分裂後 *Gcse* 由細胞核轉運至細胞質，成為頂體蛋白的一部份，頂體異常在人類會造成一種罕見的不孕症稱為 globozoospermia，發生率占不孕症病因之 0.1% (Aitken, et al., 1990)，一些頂體專一性表達基因如 *Acrosin* 突變後導致授精延緩(Adham et al.,1997)；*Gopc*(Golgi-associated PDZ and coiled-coli motif) 異常表現時，使頂體發育不全，導致 globozoospermia (Yao et al., 2002)，另外也有一些頂體蛋白陸續被發現，如 *Afaf* (Li et al., 2006b); *AEP1*(Luk et al.,2006) 及 *VAD1.2/AEP2* (Lee et al., 2008)等，但這些蛋白的功能仍未知，因此研究 Gcse 蛋白在雄性生殖細胞包括頂體之表現與功能有助於我們對於雄性生殖細胞減數分裂及頂體發育之了解。

研究方法、結果與討論（含結論與建議）

(一). *Cphx* gene

(1).**基因結構分析:** 由我們在 2006 年發表的結果(Li et al., 2006)顯示，*Cphx* 主要表現在卵細胞及胚胎幹細胞，卵巢組織中原始卵泡到成熟卵泡中的卵細胞都有 *Cphx* 基因的表現，受精卵持續表現一直到囊胚期才慢慢消失，分析 *Cphx* 基因的 mRNA 分子，發現在卵細胞成熟的過程中，*Cphx* mRNA 分子的 poly A 有延長的現象，此 mRNA 分子 poly A 延長現象可以促進 mRNA 穩定並活化轉譯作用的進行,是一些母源性基因常見的調控本身基因轉譯作用進而影響胚胎發育的機制，我們推測 *Cphx* 基因在卵細胞的成熟與早期胚胎發育過程可能扮演重要的角色。

(2).**蛋白表現**：由螢光免疫抗體分析，我們證實 Cphx 蛋白在二細胞時期表現量最高，到囊胚期後幾乎偵測不到(Cphx-Fig.1)，此結果證實 Cphx 蛋白的表現與 mRNA 的表現是相吻合的。

(3)**功能分析**:oocyte-specific RNAi，目前已得到十隻左右的 Cphx-dsRNAi 基因轉殖鼠(Cphx-Fig.2),基因轉殖母鼠 founder 其所產生的小鼠數明顯降低(Cphx-Fig.3)，大概 5-8 隻，而公鼠生殖能力不受影響，其中基因轉殖 DNA 套數較多的轉殖母鼠，其所生小鼠隻數為 4 隻左右，分析基因轉殖母鼠卵巢組織 *Cphx* 基因表現量有下降的趨勢，*Cphx* mRNA 被抑制的量由四週至十週明顯的增加，大約減少 70%，但是還是有卵細胞成熟，而且可以正常的排卵，只是前幾胎的胎數減少，同時基因轉殖母鼠有提早不孕現象，不孕小鼠之卵巢明顯的形狀不正常(Cphx-Fig.4)，分析八個月及十三個月的 Cphx-dsRNA 轉殖鼠卵巢中之濾泡發育，發現明顯的各級濾泡數目都比同齡的小鼠少了，同時濾泡的形狀也異常，甚至整個卵巢形狀也異常 (Cphx-Fig.4,5)，推測可能 *Cphx* 基因表現減少促使卵細胞成熟時間延緩，同時減少整個卵巢組織卵細胞的所有數目，因而促使細胞提早不孕

(4).在 Cphx-dsRNA 基因轉殖鼠分析結果顯示,雄性基因轉殖鼠與雌性基因轉殖鼠交配無法得到 Tg/Tg 小鼠，我們推測 *Cphx* 對於早期胚胎發育可能是必需的，當 Cphx-dsRNA 轉殖基因序列增加後，大量降低 *Cphx* 基因表現量，抑制胚胎發育，我們以顯微注射雙股 Cphx dsRNA 分析 *Cphx* 如何影響早期胚胎發育。

(5).研究 *Cphx* 基因對於卵細胞減數分裂及早期胚胎發育的影響

收集 GV oocyte 以顯微注射 c-mos 和 CphX dsRNA，注射後 24 或 48 小時觀察卵子型態,卵子進入第二次減數分裂期情況如下:CphX 組為 3.6%(3/83）;c-mos 組為 1.3%（1 /77）。對照組為 18.8%（15/ 80）;和完全未注射組為 52.4%（22/24）。在卵母細胞注射 CphX 小干擾 RNA 時，卵母細胞的數目達到第二次減數分裂階段的卵子數與對照組比較顯著下降（P <.05）(Cphx-Fig.6)。若 c-mos 及 Cphx dsRNA 注射入 2PN embryo，胚胎大

部份停在 morula 時期，只有少數進入 blastocyst (Cphx-Fig.7)。

總結與討論: *Cphx* gene 對於卵細胞的發育是必需的，當 *Cphx* 表現減少後，雖然仍有生育能力但明顯的前幾胎的胎數減少，同時 Cphx-dsRNA 轉殖鼠有提早不孕的現象，進一步分析 Cphx-dsRNA 轉殖鼠卵巢中之濾泡發育，發現明顯的各級濾泡數目都減少了，同時濾泡的形狀也異常，甚至整個卵巢形狀也異常，而在 GV oocyte 或 2PN embryo 顯微注射 CphX dsRNA 後，明顯的確實會影響減數分裂及早期胚胎之發育，因此我們推測 Cphx 基因在卵細胞發育及早期胚胎發育都扮演很重要的角色。最近的研究以生物資訊的方法也發現人類 Cphx-like 的基因，將來也可以分析不孕病人或 POF 病人，其是否有 Cphx-like 基因異常現象。

(二). *Duxbl* gene

(1). **基因結構分析:** 由我們 2010 年發表的研究結果(Wu et al., 2010)顯示 *Duxbl* 基因位於 *Cphx* 基因下游有三個重複，雖然此三個重複基因序列有 95% 的相似度，由於在 intron 4 的序列的差異，轉錄出兩種不同的 mRNA 序列 *Duxbl* 及 *Duxbl-s*，推測可產生兩種不同的蛋白，其中 Duxbl 蛋白帶有兩個同源箱區，而 Duxbl-s 則只包含了一個同源箱區 (Duxbl-Fig.1A,B)。

(2). ***Duxbl*** **基因 orthologous 分析:**小鼠雙同源箱蛋白的同源區與人類 DUX4 蛋白的相似度最高有 67%的相似度，DUX4 是目前認為與人類顏面及肩胛肱肌肉失養症(FSHD:Facioscapulohumeral Muscular Dystrophy;是第三種常見的遺傳性的肌肉萎縮症)的形成有關的基因，目前對於疾病形成的分子機制並不了解，雖然 *Duxbl* 基因由五個 exon 所組成，但人類 DUX4 基因並不包含 intron，但以同源箱區的相似度而言，可能彼此互為 orthologous (Duxbl-Fig. 1C)。

(3). Duxbl 表現分析(成熟組織):初步以 RT-PCR 的方式分析 *Duxbl* 基因的表現，成熟組織中 *Duxbl* 基因主要表現在生殖系統(卵巢組織、胎盤、子宮)及眼球組織，次要表現於腦及睪丸組織，Northern blot 結果顯示，*Duxbl* mRNA 大約 2kb 左右，與我們的 RACE 結果相符合(Duxbl-Fig.2)。

(4). Duxbl 表現分析(各個發育時期):早期胚胎發育過程，卵細胞大量表現 *Duxbl* 基因，隨著胚胎的發育一直到 17.5 天的胎兒都有 *Duxbl* 基因的表現。由於在成熟組織中卵巢組織 *Duxbl* 基因表現量相當高，因此我們進一步分析胚胎時期，不同性腺發育過程 *Duxbl* 基因的表現與分佈，發現從出生到成熟時期的卵巢組織都有 *Duxbl* 基因的表現，而相對的胚胎時期的睪丸組織開始表現 *Duxbl* 基因，出生後繼續表現，但第二週後慢慢下降到成熟時期的睪丸組織，已幾乎測不到 *Duxbl* 基因的表現(Duxbl-Fig.3)，顯示 *Duxbl* 基因以不同的調控機制影響不同性腺的發育。

(5).Duxbl 表現分析(生殖細胞):以切片原位雜交分析卵巢組織，發現 *Duxbl* 表現在卵細胞，由初始濾泡時期 (primordial follicle) 就開始表現，一直表現

到二級濾泡時期之卵石細胞都有很強之訊號(Duxbl-Fig.4B)，而睪丸組織中，*Duxbl* 基因只表現在原始精原細胞 (Duxbl-Fig.4A)，同時免疫組織染色結果也明確的指出 Duxbl 蛋白專一性的表現於不同濾泡期的卵細胞中(Duxbl-Fig.5)。

(6).Duxbl 蛋白分析：除了分析 mRNA 的表現外，由我們自己製造的 *Duxbl* 多株抗體進行免疫分析，確實在腦組織、眼球及卵巢組織中偵測到 *Duxbl* 蛋白的存在，當抗體先以 *Duxbl* 蛋白中和反應後，此抗體即失去辨識組織中 *Duxbl* 蛋白的能力，以此證實 *Duxbl* 多株抗體的專一性(Duxbl-Fig.6)。

(7).雙同源箱區功能分析：雙同源箱基因其 N 與 C 端同源箱區以大腸桿菌表達純化後，進行 DNA 結合分析發現，N 端的同源箱區具有與 DNA 結合的能力，但並沒有專一性，可以被 Poly-dI-dC 分子競爭掉，而 C 端的同源箱區卻可以專一性的結合到 TGATNNNATCA 的 palindromic 序列(Duxbl-Fig.7)(D2BS)，同時 C 端的同源箱區以 cooperative dimer 的方式結合到 D2BS，顯示兩個同源箱區可能以不同的調控機制影響下游基因的表現。

總結與討論:根據我們的研究成果顯示在小鼠胚胎發育過程中，Duxbl 蛋白主要表現於骨骼肌，但出生後隨著肌肉的發育 *Duxb*l 的表現量明顯減少，成熟的肌肉組織幾乎測不到 *Duxb1* 的表現(與人類相似)，而小鼠肌纖維母細胞株(C2C12)只有微量 *Duxb1* 基因表現，分化後的肌纖維中 Duxbl 表現明顯增加，由於正常人成熟肌肉細胞並不會表現 DUX4 蛋白，目前推測肩胛肱肌肉失養症病人肌肉細胞異常的表現 DUX4 蛋白，可能是造成疾病生成的原因，我們將進一步以小鼠 *Duxb1* 基因建立肩胛肱肌肉失養症之疾病小鼠模式，研究肩胛肱肌肉失養症之致病分子機制，除此之外 *Duxb1* 基因與眼球發育，眼外肌的形成及生殖系統的發育都有關，在生化功能上雙同源箱區在調控基因表現上，兩個同源箱區扮演不同的角色，結合不同的 DNA 序列，將來以細胞或動物為模式，進一步研究 *Duxb1* gene 調控基因表現之功能將有助於我們了解雙同源箱基因在發育及疾病(如 FSHD)的形成上所扮演的角色。

(三). *Gcse* gene

(1). Gcse 基因結構分析

Gcse 位於小鼠 14 號染色體 A3 區塊，轉錄出兩種主要的 mRNA 剪輯型式: *Gcse-l*（1589bp）與 *Gcse-s*（906bp），分別可轉譯出 215 與 152 個胺基酸序列。Gcse-l 與 Gcse-s 蛋白的 N 端 118 個氨基酸組成一致，而 Gcse-s 蛋白的 C 端有 56 個胺基酸與人類 AKT2 （Protein kinase B）的催化區域高達 50%的相似度(Gcse-Fig.1)。

(2). Gcse 基因表現的模式分析：

從 Northern blots 與 RT-PCR 實驗得知，*Gcse-l* 表現於睪丸與卵巢之中，*Gcse-s* 專一地存在於睪丸組織(Gcse-Fig.2)。以 RT-PCR，原位雜交與組織化學免疫染色分析不同發育時期的卵巢組織，發現 Gcse-l 專一表現於卵細胞

(Gcse-Fig.3),，從進入減數分裂的卵母細胞到成熟卵細胞皆有 *Gcse-l* mRNA 表現，而 Gcse-l 蛋白則從初級濾泡時期明顯增加(Gcse-Fig.4)，然而在受精卵中並未偵測到 *Gcse-l* mRNA 的表現。在睪丸組織中，*Gcse-l* mRNA 訊號從粗絲期晚期精母細胞表現到早期單倍體圓精細胞中，而 *Gcse-s* 只在早期的單倍體圓精細胞偵測到訊號(Gcse-Fig.5)。然而 Gcse-l 與 Gcse-s 的蛋白除了表現於睪丸外，其蛋白亦表現於副睪組織（成熟精子）中。藉由分離生殖細胞螢光免疫染色分析，發現 Gcse-l 蛋白存在於精母細胞核內，而在減數分裂完成的單倍體精細胞中，則發現 Gcse 蛋白會轉移頂體構造，與頂體標記蛋白－Lectin-PNA 訊號位置重疊(Gcse-Fig.6)。由 GC2(spd)細胞轉染 Gcse-l-EGFP 及 Gcse-s-EGFP，觀察到 Gcse-l-EGFP 表現於核外的 vesicle(推測為 proacrosome)，而 Gcse-s-EGFP 表現於細胞核內(Gcse-Fig.7)。

總結與討論： *Gcse* gene 屬於生殖細胞專一性表達基因，由目前的研究顯示在生殖細胞(精細胞發育)過程，其在細胞內部的表達部位 spermatogenesis 不同時期而改變，減數分裂過程中，*Gcse-l* 由核轉移至 acrosome，另外卵細胞由進入減數分裂開始至卵細胞成熟都有 Gcse-l 蛋白的表現，但受精作用後，*Gcse-l* 明顯的消失，因此推測 *Gcse-l* 在生殖細胞減數分裂過程扮演重要的角色，同時對於 acrosome 的形成是必須的，由於 Gcse-s 只在單倍體的精細胞表現，推測 *Gcse-s* 對於 spermiogenesis 可能扮演重要的角色。

參考文獻:

黃瑞喜碩士論文:小鼠雙同源箱基因(mDux)表現分佈與功能分析 (2009)

黃士玲碩士論文:新穎生殖細胞專一性表達基因(Gcse)的表達趨勢與參與精細胞頂體生成過程之探討(2010).

Wu, S.L., Tsai, M.S., Wong, S.H., Hsieh-Li, H.M., Tsai, T.S., Chang, W.T., Huang, S. L., Chiu, C.C. and **Wang, S.H.*** (2010) Characterization of Genomic Structures andExpression Profiles of Three Tandem Repeats of a Mouse Double Homeobox Gene: Duxbl Dev. Dyn. 239, 927-940.

Aitken, R. J., Kerr, L., Bolton, V., Hargreave, T., 1990. Fertil Steril. 54**,** 701-7.

Adham, I. M., Klemm, U., Maier, W. M., Hoyer-Fender, S., Tsaousidou, S., Engel, W., 1989. Eur J Biochem. 182**,** 563-8.

Choi, E., Lee, J., Oh, J., Park, I., Han, C., Yi, C., Kim do, H., Cho, B. N., Eddy, E. M., Cho, C., 2007. BMC Genomics. 8, 256.

De Rebertis, E.M. (1994) The hemeobox in cell differenitiation and evolution. In : Guidebook to the Homeobox genes, Douboule , D. (Ed) , Oxford University Press, New York , p11-23.

Galaviz-Hernandez, C., Stagg, C., de Ridder, G., Tanaka, T.S., Ko, M.S.H., Schlessinger, D. and Nagaraja, R. (2003) Gene 309: 81-89.

Gehring, W.J., Qian, Y.Q., Bileter, M., Furukbo-ToKunaga, K., Schier, A.F., Resendez-Perez, D., Affolter, M., Otting, G. and Wuthrich, K. (1994) Cell 78, 211-223.

Hong, S., Choi, I., Woo, J. M., Oh, J., Kim, T., Choi, E., Kim, T. W., Jung, Y. K., Kim, D. H.,Sun, C. H., Yi, G. S., Eddy, E. M., Cho, C., 2005. J Biol Chem. 280**,** 7685-93.

Joshi, S., Davies, H.,Sims, L.P., Levy, S.E. and Dean, J. (2006). BMC Dev Biol 7: 67-79.

Lee, K. F., Tam, Y. T., Zuo, Y., Cheong, A. W., Pang, R. T., Lee, N. P., Shum, C. K., Tam, P. C., Cheung, A. N., Yang, Z. M., Yeung, W. S., Luk, J. M., 2008. Mol Hum Reprod. 14**,** 465-74.

Li, H., Tsai, M. S., Chen, C. Y., Lian, W. C., Chiu, Y. T., Chen, G. D., Wang, S. H., 2006a. Mol Reprod Dev. 73**,** 825-33.

Li, Y. C., Hu, X. Q., Zhang, K. Y., Guo, J., Hu, Z. Y., Tao, S. X., Xiao, L. J., Wang, Q. Z., Han, C. S., Liu, Y. X., 2006b. FEBS Lett. 580**,** 4266-73.

Luk, J. M., Lee, N. P., Shum, C. K., Lam, B. Y., Siu, A. F., Che, C. M., Tam, P. C., Cheung, A. N., Yang, Z. M., Lin, Y. N., Matzuk, M. M., Lee, K. F., Yeung, W. S., 2006. J Cell Physiol. 209**,** 755-66.

Liang L, Soyal SM, and Dean J. (1997) Development 124(24):4939-4947.

MacLean, J.A., Chen, M.A., Wayne, C.M., Bruce, S.R., Rao, M., Meistrich, M.,

Macleod, C., and Wilkinson, M.F. (2005) Cell 120; 369-382.

McGinnis , W. , Levine , M.S. , Haefen , E. , Kuroiwa , A. and Gehring , W.J . (1984) Nature (London) 308, 428-433.

Qin, Y., Choi, Y., Zhao, H., Simpson, J. L., Chen, Z. J., and Rajkovic, A. (2007) Am. J. Hum. Genet 81: 576-581.

Rajkovic A, Pangas SA, Ballow D, Suzumori N and Matzuk MM. (2004) Science 305(5687):1157-1159.

Schultz, N., Hamra, F. K., Garbers, D. L., 2003. Proc Natl Acad Sci U S A. 100**,** 12201-6.

Soyal SM, Amleh A, and Dean J. (2000) Development 127(21):4645-4654.

Wang, S.H., Tsai, M.S., Chiang, M.F., and Li, H. (2003) Gene Expres. Patterns, 99-103.

Wu, S.L., Tsai, M.S., Wong, S.H., Hsieh-Li, H.M., Tsai, T.S., Chang, W.T., Huang, S. L., Chiu, C.C.and Wang, S.H. * (2010) Dev. Dyn. 239, 927-940.

Yao, R., Ito, C., Natsume, Y., Sugitani, Y., Yamanaka, H., Kuretake, S., Yanagida, K., Sato, A., Toshimori, K., Noda, T., 2002. Proc Natl Acad Sci U S A. 99, 11211-6.

附圖

Cphx-Fig.1

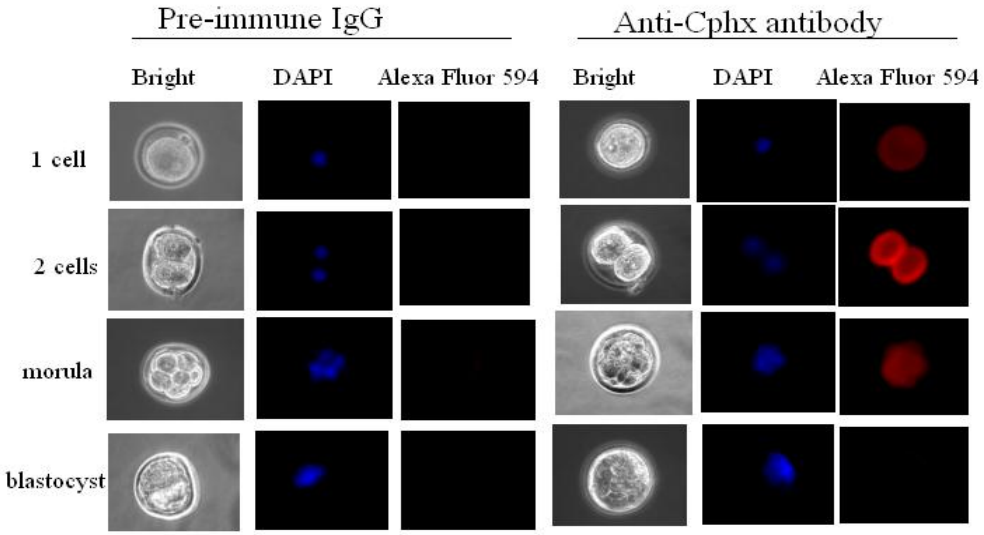

以 anti-Cphx antibody 進行螢光染色分析 Cphx 蛋白在早期胚胎發育之表現分佈，Cphx 蛋白表現量明顯的在二細胞時期表現最高，符合我們先前根據 cytoplasmic polyadenylation sequence 的推測，Cphx 屬於母源性基因，可能影響早期胚胎的發育。

Cphx-Fig.2

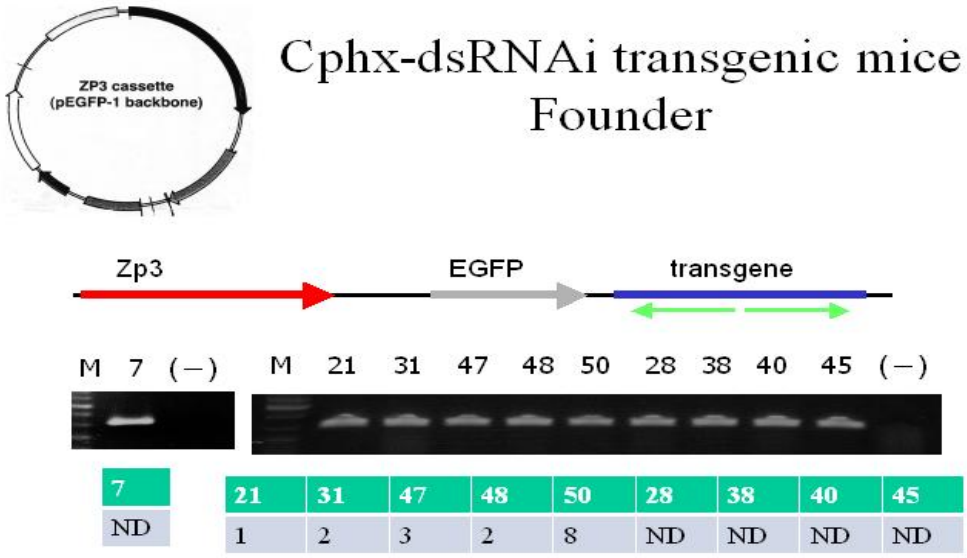

7
ND

21	31	47	48	50	28	38	40	45
1	2	3	2	8	ND	ND	ND	ND

建構以 ZP3 promoter 啟動 Cphx-dsRNA 形成之 RNAi 轉殖質體，獲得 10 隻轉殖鼠，及分析其帶有之轉殖基因套數，最高為 8 copy 之 F50 line。

Cphx-Fig.3

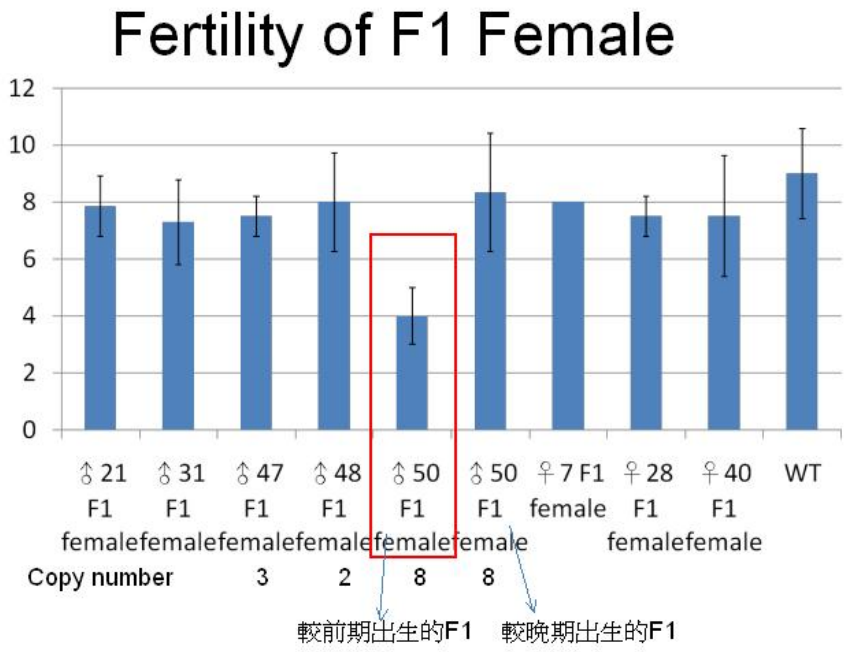

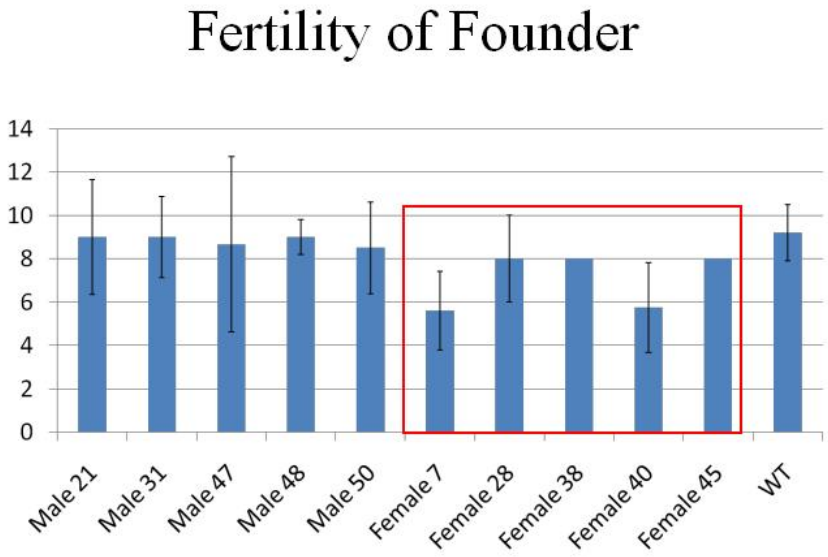

分析基因轉殖鼠 founder 及 F1 之生殖能力， 雖然 founder7,40 生殖胎數減少了，但 F1 小鼠中只有 F1-50 之生殖胎數較其它轉殖鼠少。

Cphx-Fig.4

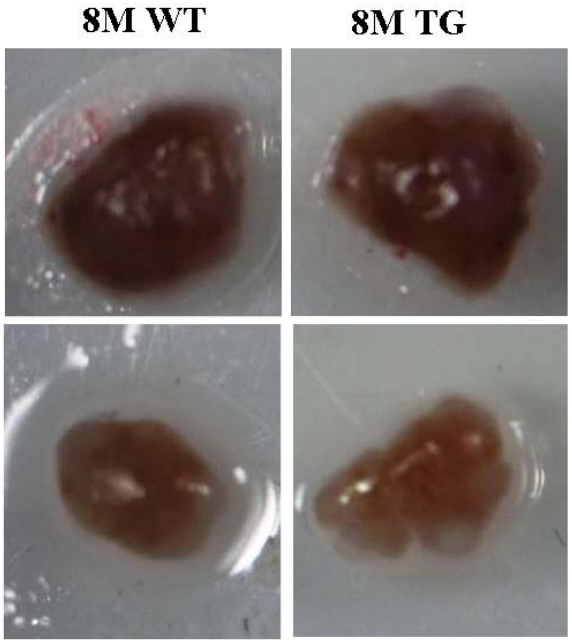

提早不孕之 TG 鼠之卵巢與仍有生育能力之同齡小鼠卵巢之比較，TG 鼠之卵巢明顯的形狀異常。

Cphx-Fig.5

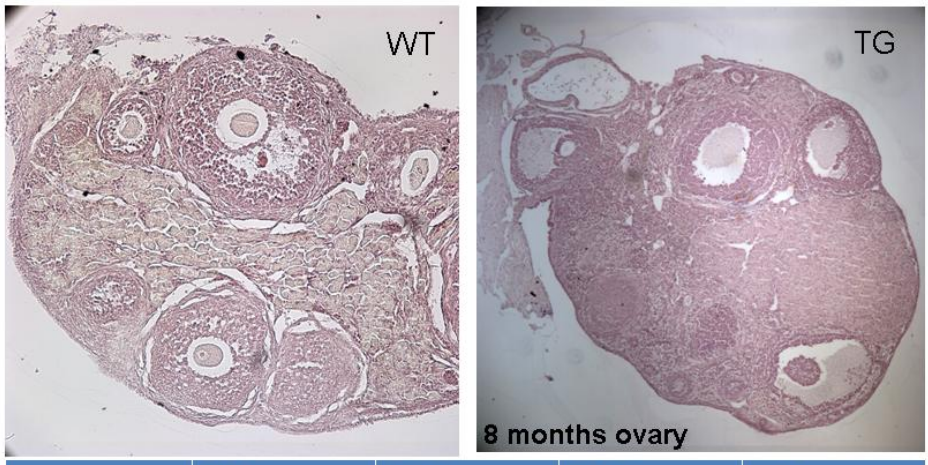

	WT 13months	TG 13months	WT 8months	TG 8months
primordial/ primary	226	186	286	232
secondary/ antral	163	150	189	148

研究發現轉殖鼠大約在八個月後就喪失生育能力，其卵巢很明顯的較 wild type 小，組織切片染色後，發現濾泡的形狀也異常，各時期濾泡數也較 wild type 少，推測 Cphx 表現量減少，可能還是影響了卵細胞或濾泡細胞的發育，使的卵巢中之卵細胞減少的較快，因此造成提早不孕。

Cphx-Fig.6

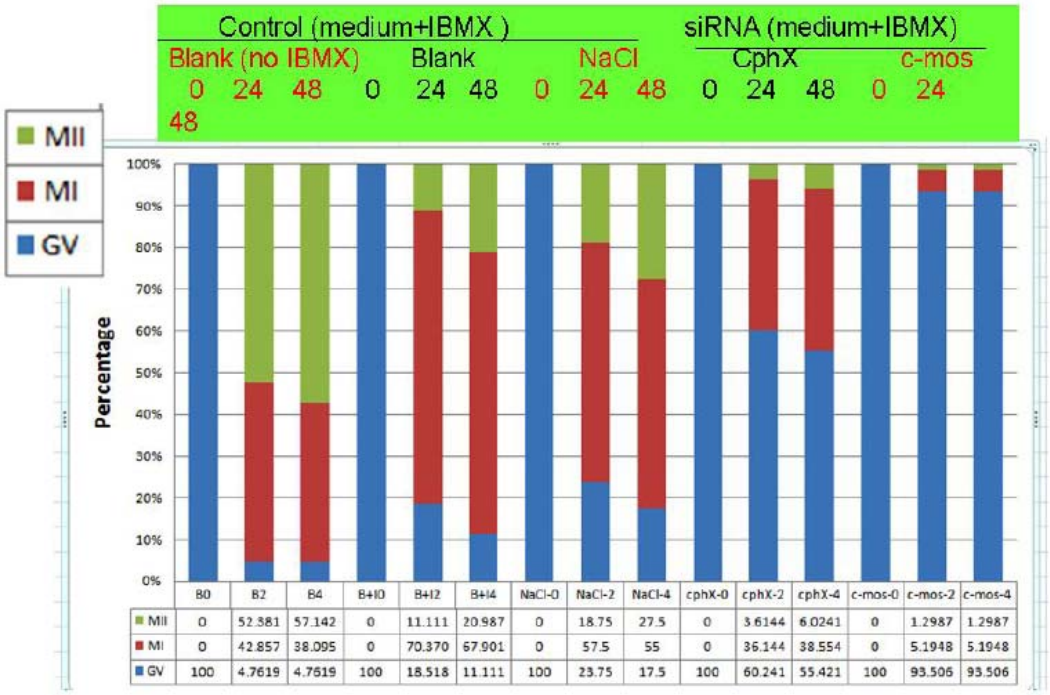

	B0	B2	B4	B+I0	B+I2	B+I4	NaCl-0	NaCl-2	NaCl-4	cphX-0	cphX-2	cphX-4	c-mos-0	c-mos-2	c-mos-4
MII	0	52.381	57.142	0	11.111	20.987	0	18.75	27.5	0	3.6144	6.0241	0	1.2987	1.2987
MI	0	42.857	38.095	0	70.370	67.901	0	57.5	55	0	36.144	38.554	0	5.1948	5.1948
GV	100	4.7619	4.7619	100	18.518	11.111	100	23.75	17.5	100	60.241	55.421	100	93.506	93.506

顯微注射 Cphx dsRNA 入 GV (germinal vesicle) oocyte，體外培養 24 至 48 小時，統計 GV 卵細胞發育至 metaphase (MI)及 metaphase II(MII)卵石細胞的數目。打入 Cphx-dsRNA 之 GV oocyte 繼續發育至 MI 或 MII 者明顯的減少 50%。

Cphx-Fig.7

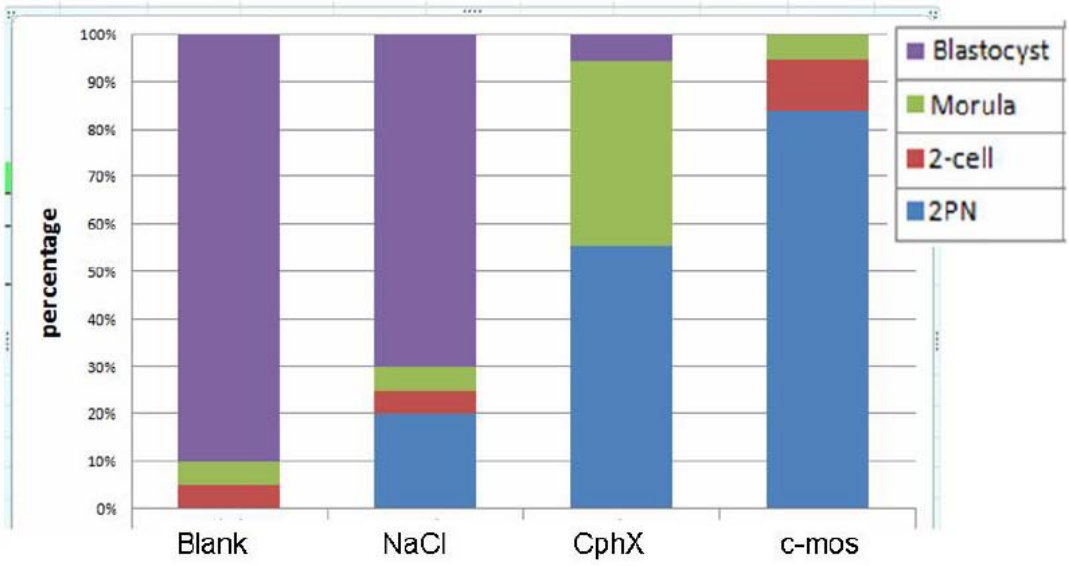

顯微注射 Cphx dsRNA 入 2PN embryo 體外培養 5 天，統計胚胎發育至 2 cell, morula 及 blastocyst 的數目。打入 Cphx-dsRNA 之 2PN embryo 繼續發育至 morula 或 blastocyst 者比 control 組少了 50 %。

Duxbl-Fig.1

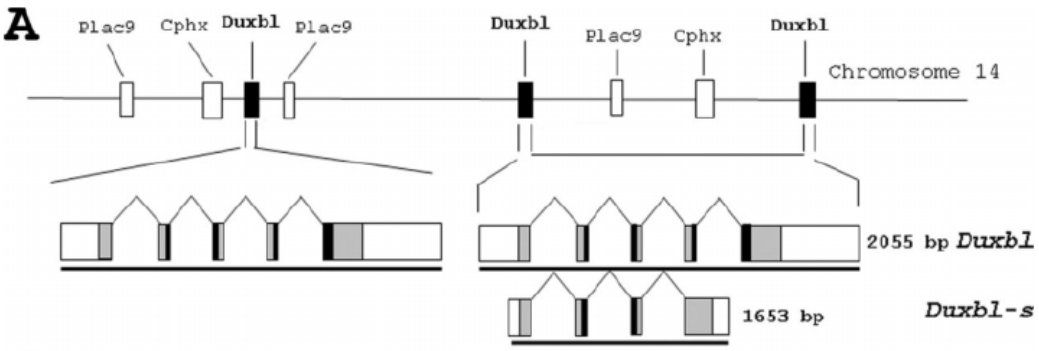

B

```
                                  Homeodomain I (H1)
Duxbl       1 MELSCSTGLLEKEARRRRIILTQSQKDTLRVWFEKNPNPDLATRGHLAKELGISESQIMT  60
Duxbl-s     1 MELSCSTGLLEKEARRRRIILTQSQKDTLRVWFEKNPNPDLATRGHLAKELGISESQIMT  60
                                                 Homeodomain II (H2)
Duxbl      61 WFQKHRKIRKQAEFACCSEESQEQEQDKPRVKEARRSRTHFTKFQTDILIEAFEKNRFPG 120
Duxbl-s    61 WFQKHRKIRKQAEFACCSEESQEQEQDKPRVKEARRSRTHFTKFQTDILIEAFEKNRFPG 120
                                  Helix 3                 Helix 1
Duxbl     121 IVTREKLAQQTGIPESRIHIWFQNRRARHPDPGQNTQKTPHPPQSSQGPTQKTVGKLAPS 180
Duxbl-s   121 IVTREKLAQQTGIPESRIHVRCASLCLWQPTCPYHKPLFSRAVDGQSQATHGCPCALDTG 180
                Helix 2

Duxbl     181 KTLTSSASVILPLSPPHTPNGPLDLSKGRQKQLPGTTLLQSSQVVQQRSDDQNPNKGHLS 240
Duxbl-s   181 CKYLVFPATVWRNSHIRPAES*                                       202

Duxbl     241 PTTTPGEQGFHSQPPLQLLTQNRGHNPRESGGLAVPRLEDCTQVPAVNQHFRKLDQNDSS 300
Duxbl-s

Duxbl     301 FLQHWDEWFGSMLAEWMPDKEYWSEKAELHPWQVQLRQLASVSPQAHQTP*           351
Duxbl-s
```

C

```
                        Helix 1          Helix 2          Helix 3          Identity
Duxbl-H1  1 ARRRRIILTQSQKDTLRVWFEKNPNPDLATRGHLAKELGISESQIMTWFQKHRKIRKQAE 60 100% (Mm)
Duxbl-H1  1 --------N--------------------------K--------------------VE 60  93% (Rn)
DUX4-H1   1 G-P--LVW-P--SEA--AC--R--Y-GI---ER--QAI--P-PRVQI---NE-SRQLRQH 60  42% (Hs)
DUXA-H1   1 H--C-TKF-EE-LKI-INT-NQK-Y-GY--KQK--L-INTE--R-QI---NR-ARHGFQK 60  35% (Hs)
DUXA-H1   1 H--C-TKF-EE-LKI-INT-NQK-Y-GY--KQK--L-INTE--R-QI---NR-ARHGFQK 60  35% (Pt)
Rax       1 H--N-TTF-TY-LHE-ERA---SHY--VYS-EE--GKVNLP-VRVQV---NR-AKWRRQE 60  32% (Mm)
Mixl      1 Q--K-TSFSSE-LQL-ELV-RQTMY--IHL-ER--ALTLLP--R-QV---NR-AKSRRQS 60  30% (Mm)
Duxbl-H2  1 ---S-THF-KF-T-I-IWA----RF-GIV--EK--QQT--P--R-HI---NR-ARHPDPG 60  43% (Mm)
                                                    *  *    *

                        Helix 1          Helix 2          Helix 3          Identity
Duxbl-H2  1 ARRSRTHFTKFQTDILIWAFEKNRFPGIVTREKLAQQTGIPESRIHIWFQNRRARHPDPG 60 100% (Mm)
Duxbl-H2  1 -G----------I----E-------------------E----------------------K 60  91% (Rn)
DUX4-H2   1 G--K--AV-GS--AL-LR----D-----AA--E--RE--L-----Q-----------GQ- 60  67% (Hs)
DUXA-H2   1 ---C--TYSAS-LHT--K--M--PY---DS--E--KEI-V----VQ-------S-LLLQR 60  53% (Hs)
DUXA-H2   1 ---C--TYSAS-LHT--K--M--PY---DS--E--KEI-V----VQ-------S-LLLQR 60  53% (Pt)
Rax       1 H--N--T--TY-LHE-ER----SHY-DVYS--E--GKVNL--V-VQV-------KWRRQE 60  45% (Mm)
Mixl      1 Q--K--S-SSE-LQL-ELV-RQTMY-D-HL--R--AL-LL-----QV-------KSRRQS 60  45% (Mm)
```

D

```
                        Helix 1          Helix 2          Helix 3          K + R
Duxbl-H1  1 ARRRRIILTQSQKDTLRVWFEKNPNPDLATRGHLAKELGISESQIMTWFQKHRKIRKQAE 60   8
Duxbl-H2  1 ARRSRTHFTKFQTDILIWAFEKNRFPGIVTREKLAQQTGIPESRIHIWFQNRRARHPDPG 60   6
DUX4-H1   1 GRPRRLVWTPSQSEALRACFERNPYPGIATRERLAQAIGIPEPRVQIWFQNERSRQLRQH 60   6
DUX4-H2   1 GRRKRTAVTGSQTALLLRAFEKDRFPGIAAREELARETGLPESRIQIWFQNRRARHPGQG 60   7
```

Fig. 1. Genomic structure and RNA transcripts of *Duxbl* genes. **A**: The tandem triplicate of mouse *Duxbl* genes and their surrounding genes (*Plac9* and *Cphx*) are present on mouse chromosome 14A3. The lengths of spaces between each *Duxbl* gene and RNA transcripts are indicated. The ORFs of *Duxbl* and *Duxbl-s* transcripts are shown in gray and the regions encoding homeodomains are in black. **B**: Comparison of the predicted amino acid sequences of Duxbl and Duxbl-s proteins. The identical amino acid residues are in bold and the homeodomains are boxed. The different amino acid residues in helix 3 of homeodomain II (H2) are in italics. **C**: Alignment of amino acid sequences of two Duxbl homeodomains (in bold) with those of other predicted homeodomains of double and paired-like homeobox genes. The names of gene products and their homeodomains are listed in the left. Dashes represent sequences identical to those of Duxbl homeodomains. Identity indicates the percentage of sequence identity to Duxbl homeodomain. The asterisks (*) indicate amino acid residues predicted to be involved in sequence-specific DNA binding. **D**: Amino acid sequences of homeodomains of human DUX4 and mouse Duxbl proteins. The basic amino acid residues in two terminal regions of homeodomains are shown in bold. The total numbers of lysine and arginine residues in two ends are shown on the right.

Duxbl-Fig.2

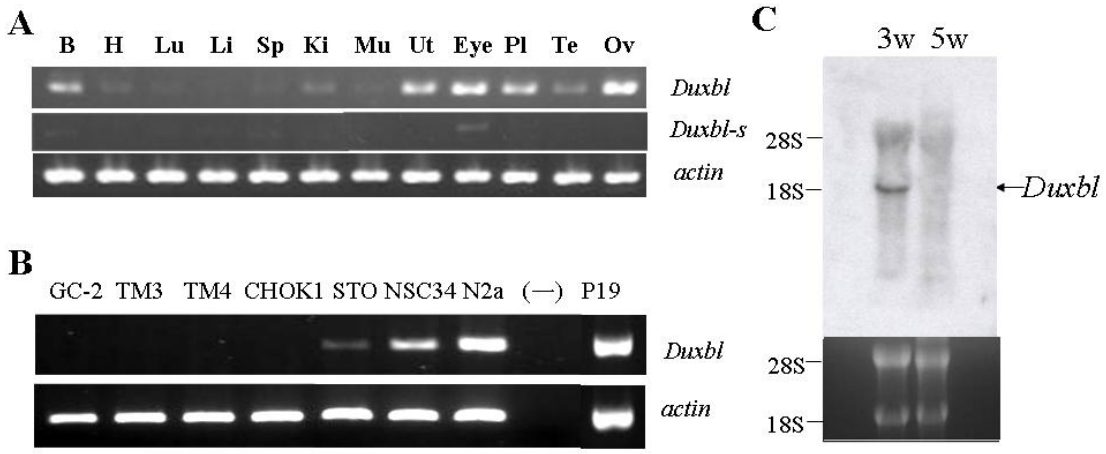

(A) 以 RT-PCR 分析 Duxbl 及 Duxbl-s 在各組織器官之表現，生殖系統的組織如卵巢、睪丸、子宮、胎盤及眼球、腦組織都有 Duxbl 基因之表現。

(B) 以 RT-PCR 分析 Duxbl 及 Duxbl-s 在各細胞株之表現，NSC34, N2A 及 P19 表現量最高。

(C) 取 3w 及 5w 之小鼠 testis 進行 northern blot 分析 Duxbl 基因之表現，在 3w 明顯的有 2kb 左右的訊號出現。

Duxbl-Fig.3

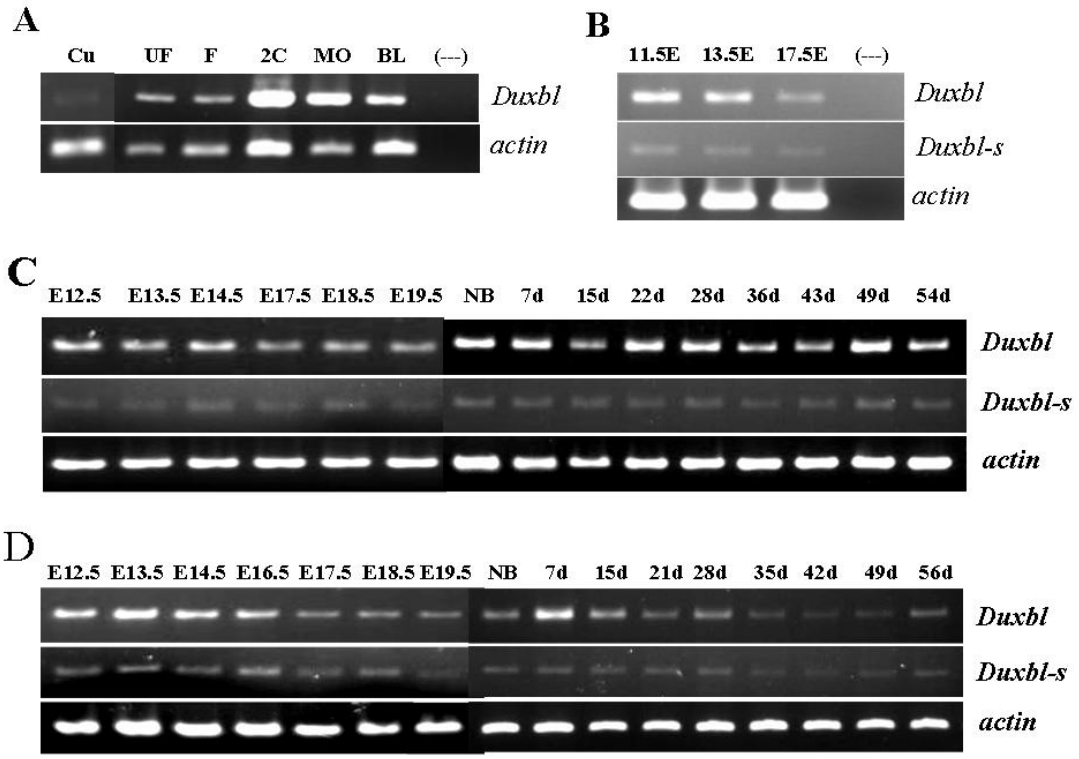

(A). RT-PCR 分析早期胚胎 *Duxbl* 基因之表現，由成熟卵細胞開始到受精後，早期胚胎之發育，Duxbl 都持續性的表現。

(B). RT-PCR 分析 11.5, 13.5,17.5 小鼠胚胎 *Duxbl* 基因之表現，都有 Duxbl 基因之表現。

(C). RT-PCR 分析胚胎時期及出生後到成熟時期卵巢組織 *Duxbl* 基因之表現，由胚胎時期開始，卵巢進入減數分裂時期

(D). RT-PCR 分析胚胎時期及出生後到成熟時期睪丸組織 *Duxbl* 基因之表現

Duxbl-Fig.4

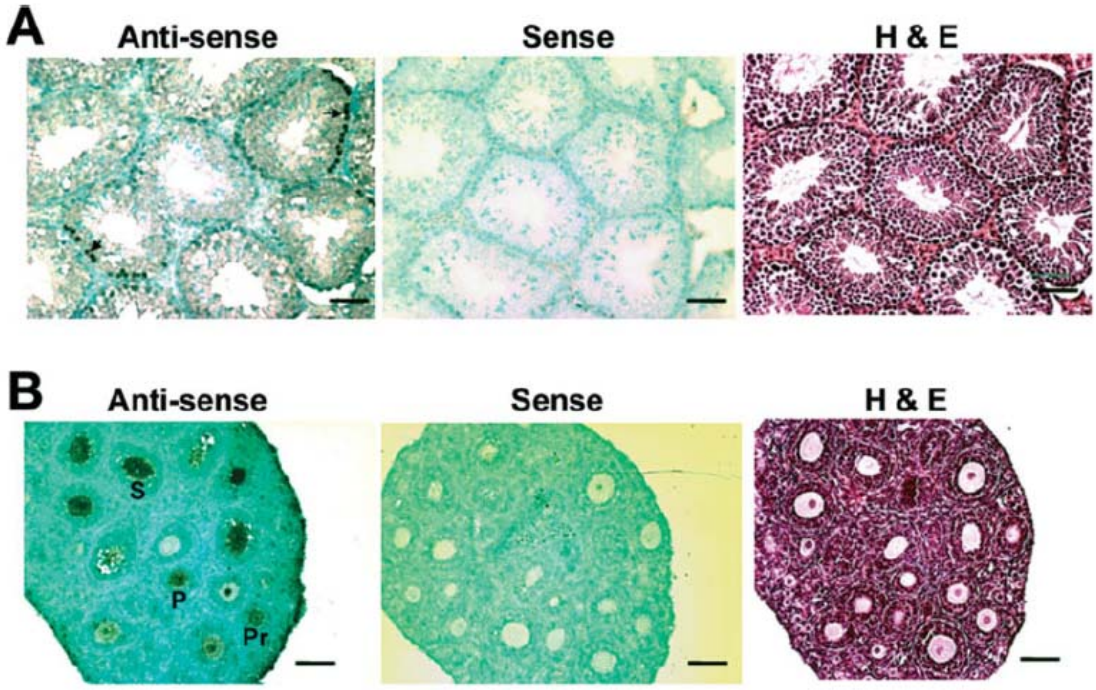

(A). 以 in situ hybridization 分析 *Duxbl* 在睪丸組織之表現，*Duxbl* 表現在精原細胞 (spermatogonia)。

(B). 以 in situ hybridization 分析 *Duxbl* 在卵巢組織之表現，*Duxbl* 表現於 primodial, primary 及 secondary follicle 中之卵細胞 。

Duxbl-Fig.5

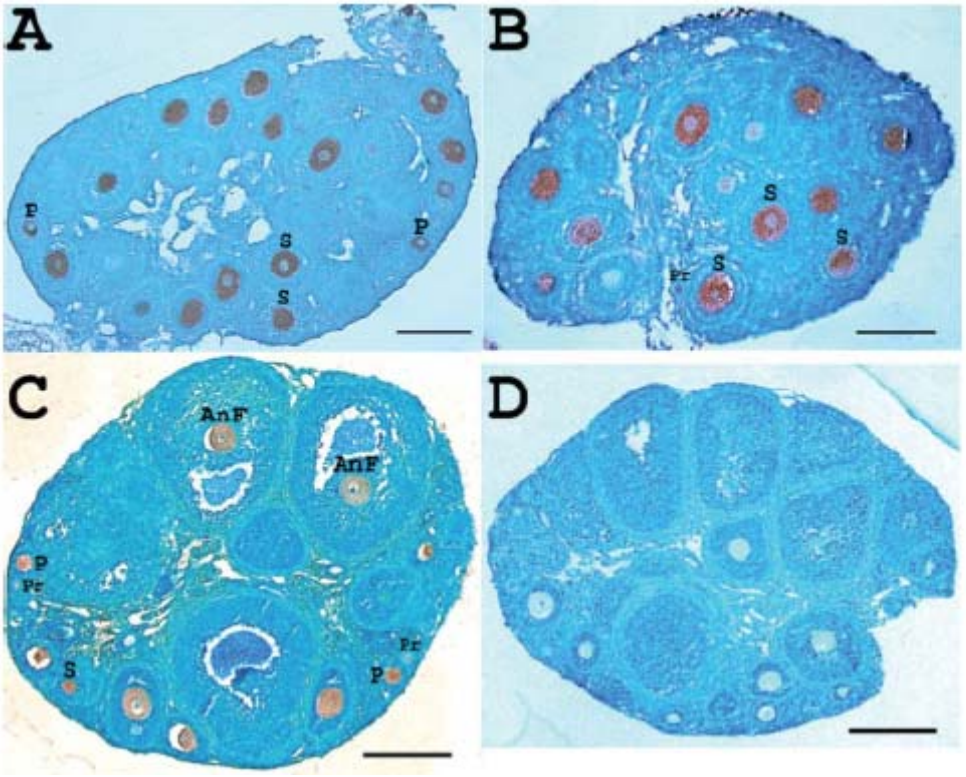

以免疫組織染色法分析 Duxbl 蛋白在卵巢組織之表現，Duxbl 蛋白專一性的表現於 primodial, primary, secondary, antral follicle 中之卵細胞中。

Duxbl-Fig.6

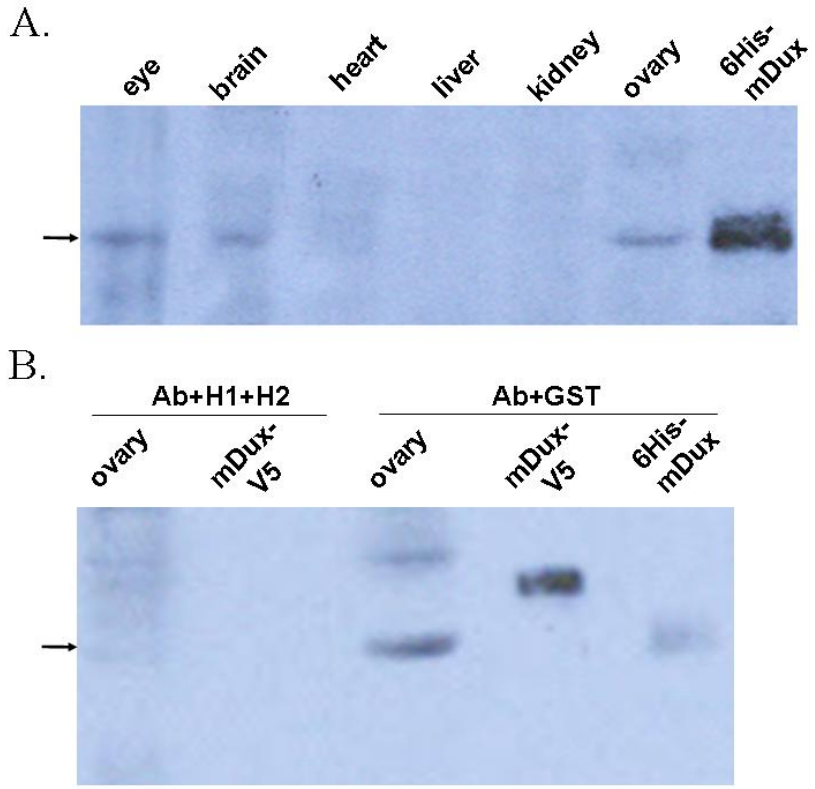

(A).以自製 Duxbl 抗體 分析成熟組織中 Duxbl 蛋白之表現
(B).以純化之 GST-H1 及 GST-H2 蛋白中和 Duxbl 抗體，分析自製 Duxbl 抗體是否專一的辨識 Duxbl 蛋白，Duxbl 抗體以 GST-H1 及 GST-H2 中和後，無法辨識組織及 E.coli 表現之 Duxbl 蛋白。

Duxbl-Fig.7

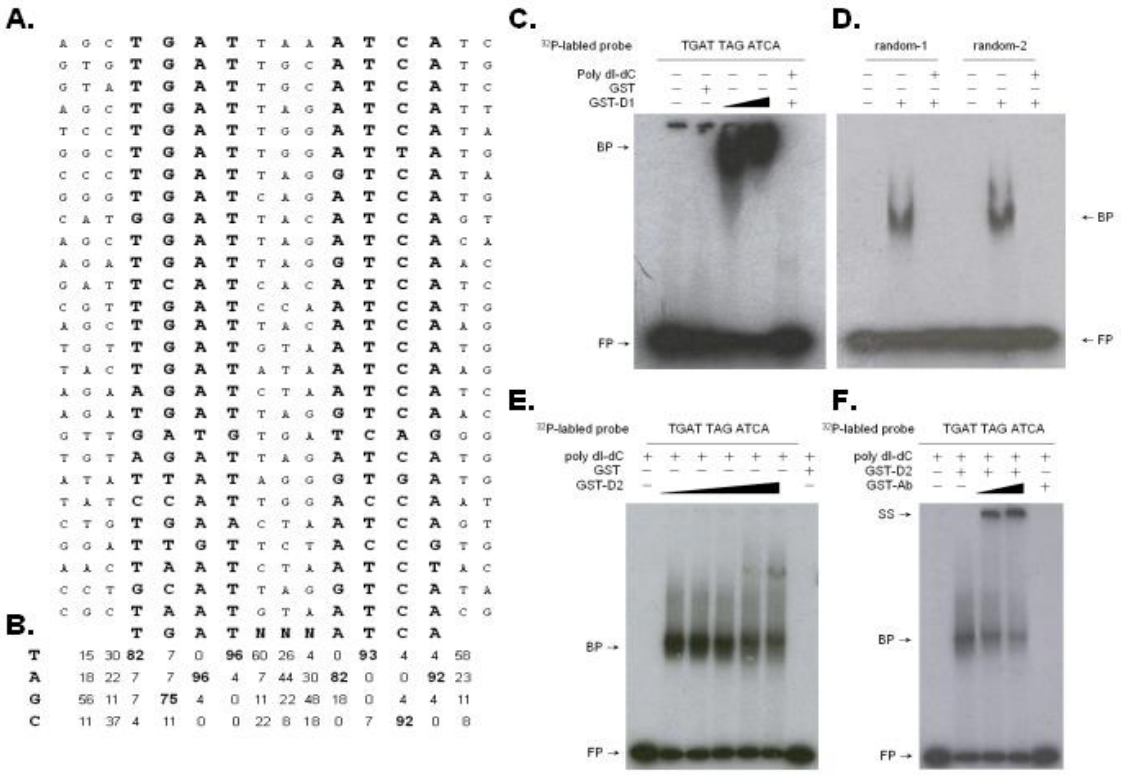

(A,B).以 **Cyclic Amplification of Sequence Target (CAST) assay 找出 Duxbl homeodomain II 之結合序列為 TGATNNNATCA** palindromic 序列(D2BS)

(C,D,E,F).以 EMSA assay 證實 homeodomain II 與 D2BS 具有專一性的結合能力

Gcse-Fig.1

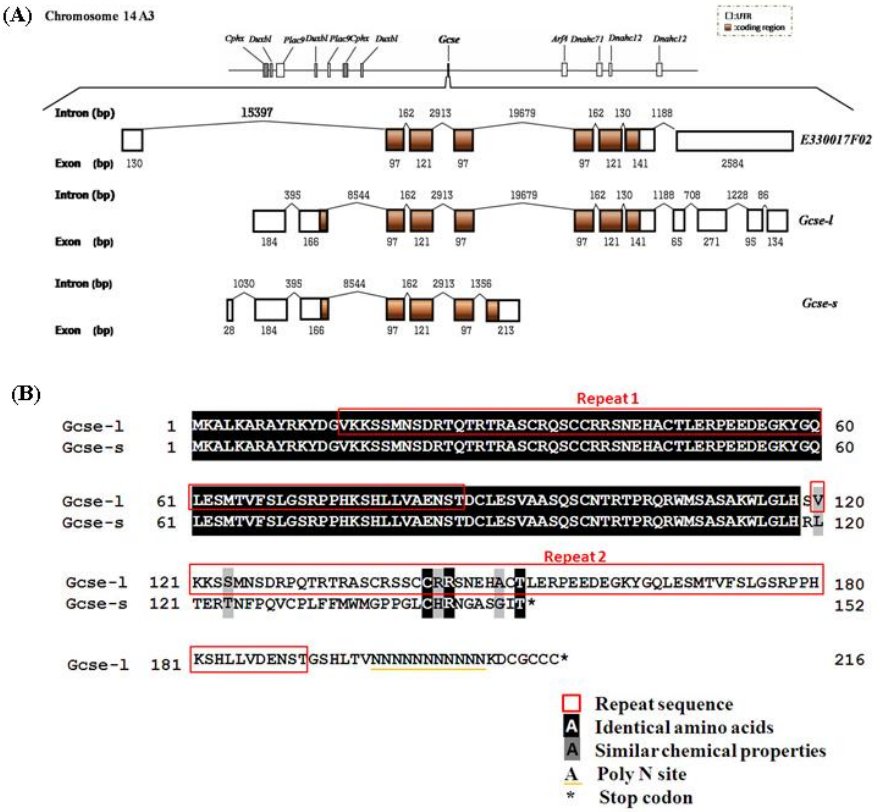

Gcse 基因結構分析及推測之氨基酸序列

（A）*Gcse* 兩種轉錄形式的外顯子-內插子的分佈圖。白色區域為非轉譯區，棕色所示為轉譯區。紅色底線代表DNA 的重複片段。

（B）Gcse-1 與Gcse-s 之胺基酸比對：以數字標記每段胺基酸之數目，Gcse-1 與Gcse-s N 端前118 個胺基酸完全相同（黑色方框）。Gcse-1 有71 個胺基酸重覆（紅色方框），C 端有連續11 個天門冬醯胺（Asparagine，N；黃色底線）。灰色為性質相同之胺基酸。

（C）*Gcse* 同源基因比對：Gcse-s 有一段序列（56 個胺基酸）與人類Akt2（Protein Kinase B）催化區域相似度高達50%，而Gcse-1 相似度為39%。

Gcse-Fig.2

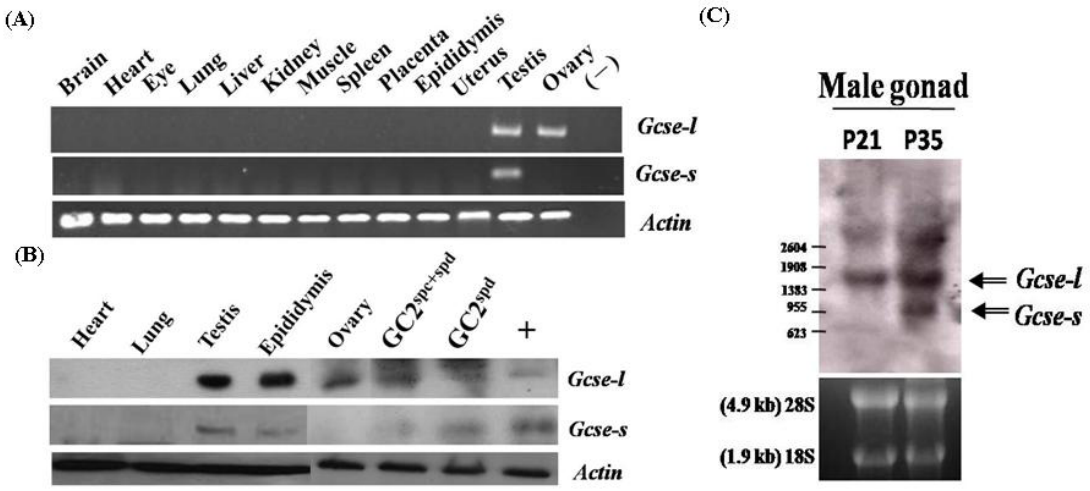

(A) 以2μg之RNA 進行RT-PCR分析*Gcse* mRNA在小鼠各組織表現分佈。

(B) 以西方點墨法測試抗體辨識內生性Gcse蛋白能力。Heart：心臟，Lung：肺臟，epididymis：副睪，GC2spc＋spd：精母細胞與圓精細胞，GC2spd：圓精細胞。Actin為internal control。+：Gcse-V5-6His重組 蛋白。

(C). 經由北方點墨法分析Gcse mRNA的表現，以25μg之testis RNAs進行偵測，得知Gcse-l分子量大約1.589 kb，Gcse-s分子量大約906 bp。 rRNA 28S與18S當為internal control，並以RNA marker作為判斷分子量之標準品。

Gcse-Fig.3

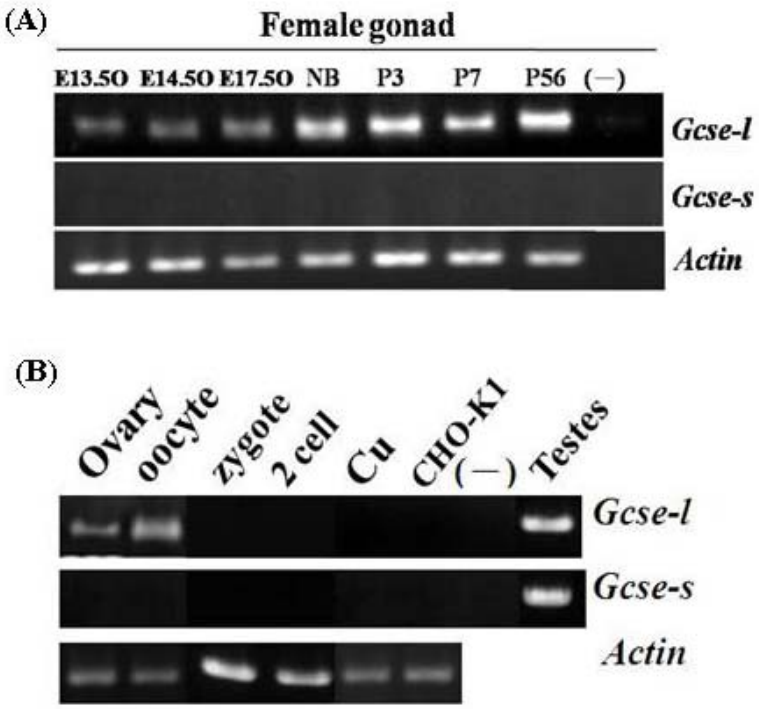

Gcse mRNA在不同發育時期之小鼠卵巢組織與著床前胚之表現

(A) 以2μg之卵巢RNA 進行RT-PCR，分析卵巢不同發育時期之Gcse基因表現。*Actin*為 internal control。E13.5O- E17.5O：胚胎時期卵巢，NB：new-born ovary；P3-P56：出生後（postnatal）不同天數之卵巢。

(B) 以RT-PCR分析成熟卵細胞（oocyte），合子（zygote）、兩細胞時期（2-cell stage）、卵丘細胞（Cu：cumulus cells）與CHO-K1中*Gcse*的表現，各取50顆卵細胞與受精卵進行反轉錄。

Gcse-Fig.4

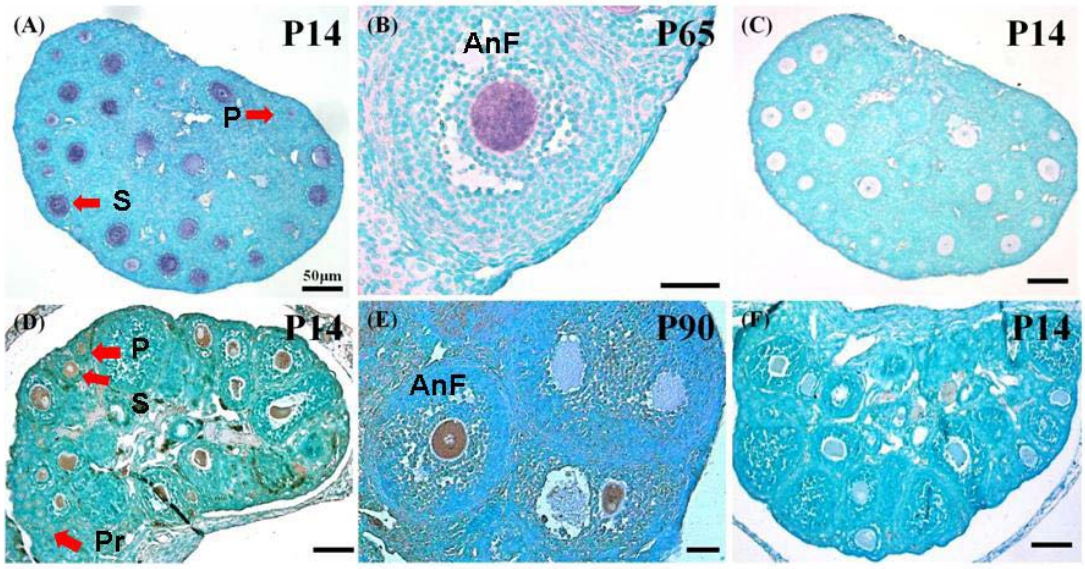

切片原位雜交及免疫組織染色分析*Gcse-1* mRNA及蛋白在卵巢組織之表現

(A－B) 利用antisense *Gcse-1*探針與卵巢組織切片進行原位雜交，紫色訊號為*Gcse-1*表現訊號。(C)利用sense *Gcse-1*探針作為控制組

(D-E) 以實驗室自製之Gcse抗體，針對出生14、35與90天之小鼠卵巢組織切片進行免疫組織染色。棕色訊號為Gcse-1蛋白質訊號。(F)免疫前IgG抗體作為對照組。 Pr：原始濾泡、P：初級濾泡、S：次級濾泡與。Anf：腔室濾泡。P14、P65：小鼠出生後14、65天

Gcse-Fig.5

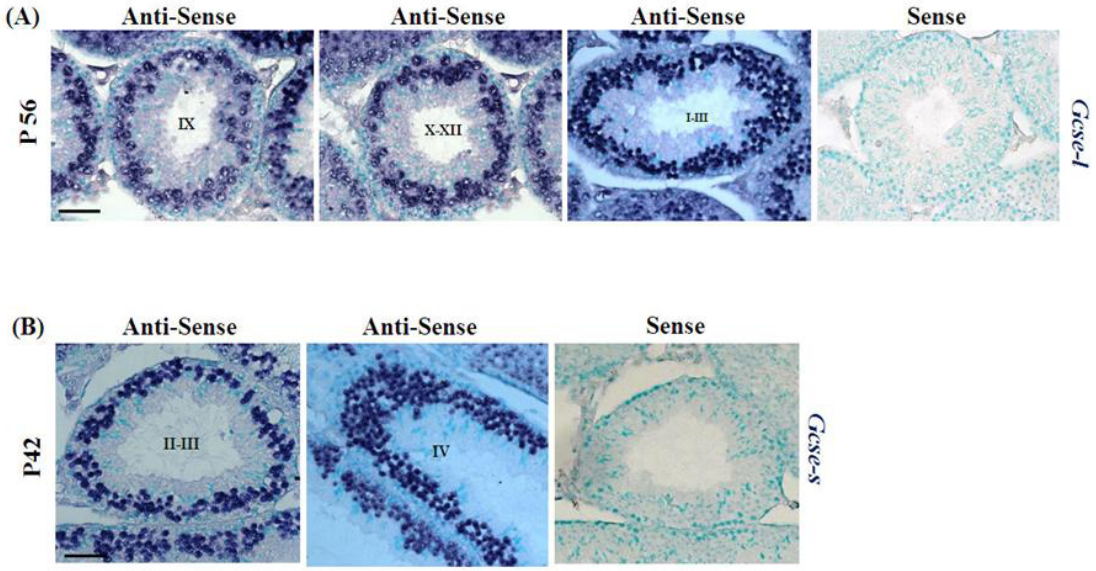

切片原位雜交分析*Gcse-l* 與*Gcse-s* mRNA在睪丸組織之表現

(A-B) 將成鼠睪丸組織連續切片，利用antisense *Gcse-l*及*Gcse-s* 探針與組織進行原位雜交，HE染色確認細胞型態與細精管時期，黑紫色訊號為*Gcse*訊號，sense 探針作為對照組。P42、56：出生後42、65天；scale bar：50 μm。

Gcse-Fig.6

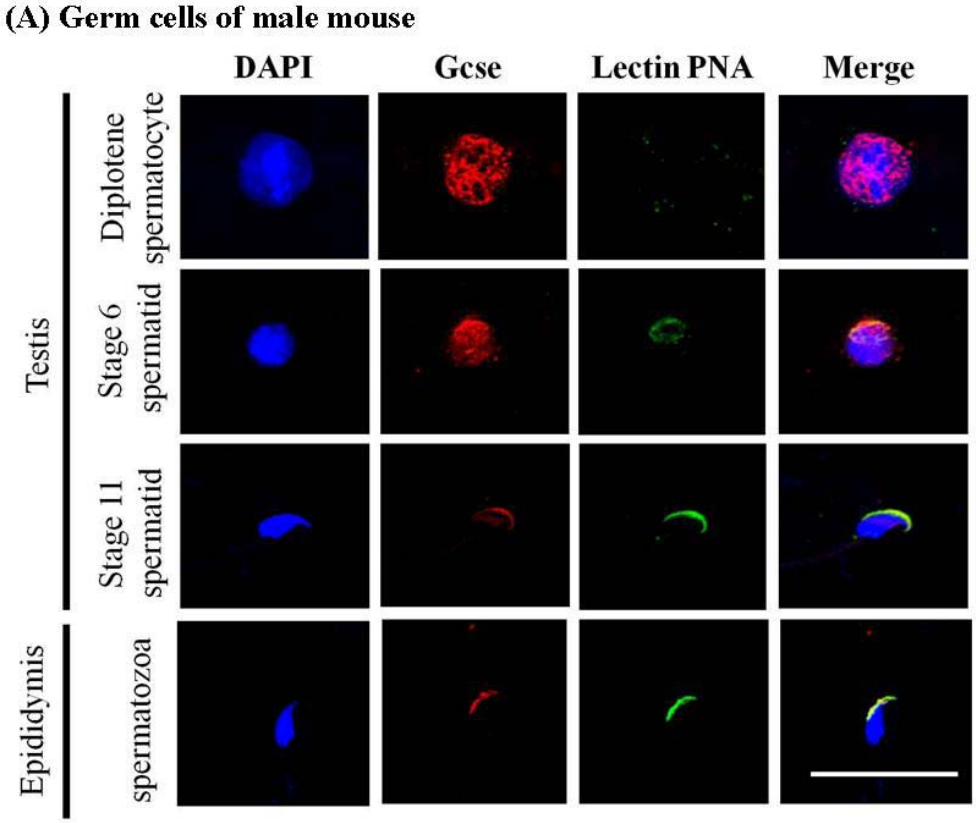

將成鼠睪丸與副睪細精管破壞，分離生殖細胞，以細胞螢光免疫染色法分析內生性之Gcse 蛋白表現。利用Gcse 抗體辨認Gcse，再以紅色螢光標定Gcse 抗體，綠色螢光標定頂體膜蛋白lectin-PNA，DAPI 染細胞核。scale bar：50μm

Gcse-Fig.7

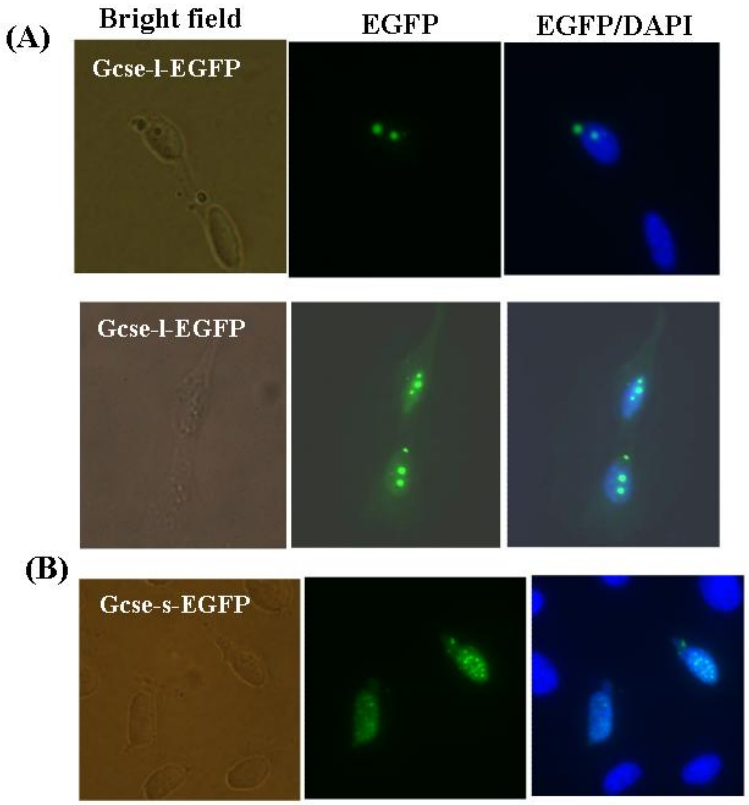

將Gcse-l-EGFP或 Gcse-s-EGFP 送入GC2 cell，觀察EGFP螢光表現部位，由圖(A)Gcse-l-EGFP表現在核外，而且以vesicle的形式存在，推測形成proacrosome，圖(B).Gcse-s-EGFP表現在細胞核內。

附件二

國科會補助專題研究計畫成果報告自評表

1. 請就研究內容與原計畫相符程度、達成預期目標情況作一綜合評估

■達成目標

□ 未達成目標（請說明，以 100 字為限）

□ 實驗失敗

□ 因故實驗中斷

□ 其他原因

2. 研究成果在學術期刊發表或申請專利等情形：

論文：■已發表 □未發表之文稿 ■撰寫中 □無

專利：□已獲得 □申請中 □無

技轉：□已技轉 □洽談中 □無

其他：(以 100 字為限)

3. 請依學術成就、技術創新、社會影響等方面，評估研究成果之學術或應用價值（簡要敘述成果所代表之意義、價值、影響或進一步發展之可能性）

本研究發現兩個新穎生殖細胞專一性表達基因 *Cphx* 及 *Gcse*，及一個人類 FSHD 疾病致病基因 DUX4 之同源基因 *Duxbl*，其中 *Cphx* 以 RNAi 技術分別以基因轉殖及體外 microinjection 的方式降低 *Cphx* 基因的表現，研究發現 Cphx-dsRNA 轉殖鼠生殖能力降低，同時提早不孕，而 microinjection Cphx dsRNA 也影響卵細胞的成熟與早期胚胎發育，我們推測 *Cphx* 基因影響卵細胞成熟發育及早期胚胎之發育， *Cphx* 基因之研究，在學術上可以幫助我們了解複雜的生殖細胞發育機制，在社會影響方面同時也可以幫助我們解開人類不孕症與卵巢提早老化之謎，將來進一步找出人類 *CPHX* 基因，同時分析不孕症病人或卵巢提早老化病人其 *CPHX* 基因是否異常，將有助我們了解不孕症之成因。另外一個生殖細胞專一性表達基因 *Gcse*，根據我們的結果顯示，與生殖細胞減數分裂及 acrosome 的形成有關，減數分裂正常與否將影響單倍體生殖細胞之合成，而 acrosome 是受精作用必要的胞器，是決定精細胞與卵細胞結合之重要構造，因此，對 *Gcse* 基因的研究將有助於我們對單倍體生殖細胞之產生與受精作用的了解，對於不孕症病人生殖細胞數目為何異常及為何精細胞無法與卵細胞結合有更進一步的了解，最後一個基因 *Duxbl* 雖然也表現於生殖細胞，但也表現於骨骼肌，更重要的是人類 FSHD 疾病致病基因 DUX4 之同源基因，對 *Duxbl* 的研究將有助於我們了解骨骼肌發育及 FSHD 之致病機制，進而找到 FSHD 治療的方法，目前我們的研究顯示 *Duxbl* 基因異常的表現將抑制肌纖維的分化，無法形成多核的肌小管，根據我們 *Duxbl* 基因之研究成果，將來可以建立 FSHD 疾病的小鼠模式，將可以協助我們進一步了解 FSHD 致病機制及找出治療 FSHD 疾病的方法。

Characterization of Genomic Structures and Expression Profiles of Three Tandem Repeats of a Mouse Double Homeobox Gene: *Duxbl*

Shey-Lin Wu,[1†] Ming-Shiun Tsai,[2†] Swee-Hee Wong,[3] Hsiu-Mei Hsieh-Li,[4] Tz-Shiu Tsai,[3] Wei-Tang Chang,[3] Shin-Ling Huang,[3] Chun-Ching Chiu,[1] and Sue-Hong Wang[3,5]*

We identified and cloned a mouse double homeobox gene (*Duxbl*), which encodes two homeodomains. *Duxbl* gene, a tandem triplicate produces two major transcripts, *Duxbl* and *Duxbl-s*. The amino acid sequences of Duxbl homeodomains are most similar to those of human DUX4 protein, associated with facioscapulohumeral muscular dystrophy. In adult tissues, *Duxbl* is predominantly expressed in female reproductive organs and eyes, and slightly expressed in brain and testes. During gonad development, *Duxbl* is expressed from embryonic to adult stages and specifically expressed in oocytes and spermatogonia. During embryonic development, *Duxbl* is transcribed in limbs and tail. However, Duxbl proteins were only detected in trunk and limb muscles and in elongated myocytes and myotubes. In C2C12 muscle cell line, *Duxbl* expression pattern is similar to differentiated marker gene, *Myogenin*, increased in expression from 2 days onward in differentiating medium. We suggest that Duxbl proteins play regulatory roles during myogenesis and reproductive developments. *Developmental Dynamics 239:927–940, 2010*. © **2010 Wiley-Liss, Inc.**

Key words: double homeobox gene; Duxbl; myogenesis; reproductive development; mouse embryo

Accepted 28 November 2009

INTRODUCTION

Homeobox genes encode transcription factors that regulate embryonic development programs including organogenesis, axis formation, and limb development (McGinnis and Krumlauf, 1992; Boncinelli, 1997). Their products regulate the expressions of target genes in tissue- and spatiotemporal-specific manners through conserved DNA-binding motifs called homeodomains. Homeodomains have three α-helical segments of which the third constitutes the main DNA recognition site and binds to the major groove of DNA (Gehring et al., 1994). This sequence-specific binding allows homeodomain proteins to activate or repress the expression of a battery of downstream target genes. The correct expressions of homeodomain proteins in adult tissues including liver, kidney, and intestine are important for the regulations of cellular morphogenesis, growth, and differentiation (Cillo et al., 2001).

Different homeobox genes are classified through similarities in amino acid sequences within their homeodomains and the other coding regions of their gene products (Galliot et al., 1999; Holland and Takahashi, 2005). The *paired* (PRD) class is divided into two subclasses: the *PAX* subclass and the *PAXL* subclass (Holland et al., 2007). The *PAX* subclass homeodomain proteins have a conserved 130-amino-acid DNA-binding domain, the paired domain, upstream of their homeodomains (Bopp et al., 1986). The *PAX* gene family is an ancient and remarkably conserved gene family, which plays key roles in the formations of tissues and organs during embryogenesis. *PAX3* and *PAX7* mark myogenic progenitor cells and

[1]Department of Neurology, Chang-Hua Christian Hospital, Changhua, Taiwan
[2]Department of Bioindustry Technology, Da-Yeh University, Dacun, Changhua, Taiwan
[3]Department of Biomedical Sciences, Chung Shan Medical University, Taichung, Taiwan
[4]Department of Life Science, National Taiwan Normal University, Taipei, Taiwan
[5]Department of Medical Research, Chung Shan Medical University Hospital, Taichung, Taiwan
Grant sponsor: National Science Council of Taiwan. ROC; Grant number: NSC 97-2320-B-040-010-MY3; Grant number: 97-CCH-CSMU-15.
†**Drs. S-L Wu and M-S Tsai contributed equally to this work.**
***Correspondence to: Sue-Hong Wang, Department of Biomedical Sciences, Chung Shan Medical University, No. 110, Sec. 1, Jianguo N. Road, Taichung 402, Taiwan. R.O.C. E-mail: wangsh@csmu.edu.tw**

DOI 10.1002/dvdy.22210
Published online 8 January 2010 in Wiley InterScience (www.interscience.wiley.com).

regulate their behaviors and entries into the program of skeletal muscle differentiation (Buckingham and Relaix, 2007). *PAX6* is required for eye formation in vertebrates and its homologues in invertebrates, such as *eyeless* in *Drosophila* also play a crucial role in eye formation (Kozmik, 2005). The *PAXL*-subclass homeodomain proteins show significant sequence similarities (55–75%) to PRD-class homeodomain proteins but lack the paired domain, and contain a glutamine residue at position 9 of the third helix in their homeodomains (Burglin, 1994). Another common feature of *PAXL* homeobox genes is the presence of an additional intron within their homeoboxes, between the region that encodes position 46 and 47 homeodomain amino acid residues. Many *PAXL* homeobox genes, such as *Rax* (retinal homeobox), *Arx* (aristaless-related homeobox), and *Vsx* (visual system homeobox), are expressed in the nervous system and during brain or eye morphogenesis (Mathers et al., 1997; Miura et al., 1997; Ohtoshi et al., 2001). They play critical roles during embryonic developments.

The human double homeobox (*DUX*) genes encode two *PAXL*-subclass homeodomains. The *DUX* genes are present in multiple polymorphic copies with a 3.3-kilobase (kb) tandem repeat scattered in human heterochromatins (Ding et al., 1998; Gabriels et al., 1999; Beckers et al., 2001). The 3.3-kb dispersed *DUX* repeats in the D4Z4 locus of chromosome 4 (*DUX4*) have been found to be associated with the facioscapulohumeral muscular dystrophy (FSHD), the third most common form of inherited muscular dystrophy (Wijmenga et al., 1992; van Deutekom et al., 1993; Hewitt et al., 1994). It has been hypothesized that the larger *DUX4* copy numbers in nonaffected individuals are associated with an inhibitory chromatin structure preventing gene expressions, and the inhibition is relieved by the shorter *DUX4* arrays found in FSHD patients (Winokur et al., 1994; Tupler and Gabellini, 2004). The coding region of human *DUX4* gene shows evolutionary conservation (Clapp et al., 2007) and DUX4 protein can be detected in primary myoblasts extracted from FSHD patients (Belayew, 2004; Kowaljow et al., 2007). Previously, DUX4 protein is identified to have pro-apoptotic activity (Kowaljow et al., 2007) and is found to be a transcriptional activator of *PITX1* gene (Dixit et al., 2007). DUX4 expression recapitulates key features of FSHD molecular phenotype, including repression of MyoD and its target genes, and then diminished myogenic differentiation (Bosnakovski et al., 2008). However, the mechanism(s) that causes FSHD phenotype remain unclear. Furthermore, the in vivo functions of DUX4 protein, especially in normal tissues, remain unknown. Other human double homeobox genes are previously identified using *PRD*-class homeoboxes as query sequences to search human genome sequences, and they have been assigned into four paralogous groups including *DUXA*, *DUXB*, *DUXC*, and *DUXB*-like (*Duxbl*; Booth and Holland, 2007; Clapp et al., 2007). The molecular structures of their transcripts and the expression patterns and functions of their protein products have not been provided.

Recently, a novel mouse double homeobox gene has been reported as *Duxl* (Kawazu et al., 2007) and *Duxbl* (Clapp et al., 2007), respectively. This gene has been shown to play a critical role in CD4/CD8 double negative thymocyte development (Kawazu et al., 2007), but its detailed genomic structure, major transcript(s), expression patterns, and protein product(s) are not available. Here, we characterize the genomic structure of this mouse double homeobox gene, *Duxbl*, and suggest that the *Duxbl* gene is the mouse ortholog of human *DUX4* gene. The Duxbl protein is found expressed in adult tissues, including reproductive tissues, eyes, brain, but not in muscle. However, during embryo development, Duxbl is seen expressed in differentiated myocytes. The spatiotemporal expression patterns of *Duxbl* are also analyzed during gonad developments, and *Duxbl* is specifically expressed in germ cells, including oocytes and spermatogonia. Duxbl is predicted to play important regulatory roles during myogenesis and reproductive developments.

RESULTS AND DISCUSSION

Genomic Structure and RNA Transcripts of *Duxbl* Genes

To identify novel homeobox genes involved in early embryonic development, we screened a murine embryonic stem cell cDNA library by degenerate RT-PCR (Wang et al., 2003; Li et al., 2006). One of the genes identified contained a sequence similar to a Riken full-length cDNA clone (1110051B16 Rik) previously reported as *Duxl* (Kawazu et al., 2007) and *Duxbl* (Clapp et al., 2007), respectively. However, the genomic structure, expression profiles, protein product(s) of this gene, and in vivo function(s) of this gene product(s) are all unknown. Based on the sequence in the database (1110051B16Rik), the putative translated protein of this gene, *Duxbl*, contains two helix-turn-helix domains weakly similar to the known homeodomains. Analysis of the genomic structure of *Duxbl* gene based on information in Ensembl and NCBI databases localized it to the mouse chromosome 14A3, downstream of the *Cphx* gene (previously named as *Eso-1*, Li et al., 2006) and mapped to 24.82m (Gene ID: 48502; Fig. 1A). However, we discovered two other downstream *Duxbl* genes mapped to 24.96m (Gene ID: 72675) and 25.1m (Gene ID: 72672; Fig. 1A). These two downstream *Duxbl* genes are identical to each other, and share approximately 95% sequence identity with the upstream one (Gene ID: 48502). During analysis of the genomic structure of *Duxbl*, we observed that in addition to *Duxbl*, *Plac9*, and *Cphx* genes in mouse chromosome 14A3 are all duplicated. Previous reports suggested that *Plac9* and *Cphx* genes play important roles in mouse reproduction (Galaviz-Hernandez et al., 2003; Li et al., 2006). This near-telomeric cluster of reproductive genes in rodents may constitute an evolutionary advantage (Paillisson et al., 2005) and may come from a mechanism for protecting genes against mutation (Clapp et al., 2007). The location of these *Duxbl* genes in a near-telomeric cluster neighboring two reproductive genes (*Plac9* and *Cphx*) suggests that *Duxbl* genes also play a role in mouse reproduction.

According to our data of rapid amplification of cDNA ends (RACE) and the sequences of expressed sequence tag (EST) clones in databases, the upstream *Duxbl* gene (Gene ID: 48502) is composed of five exons spanning 6,390 bp. More than one transcriptional start sites for this *Duxbl* were identified by 5′ RACE analysis. The major

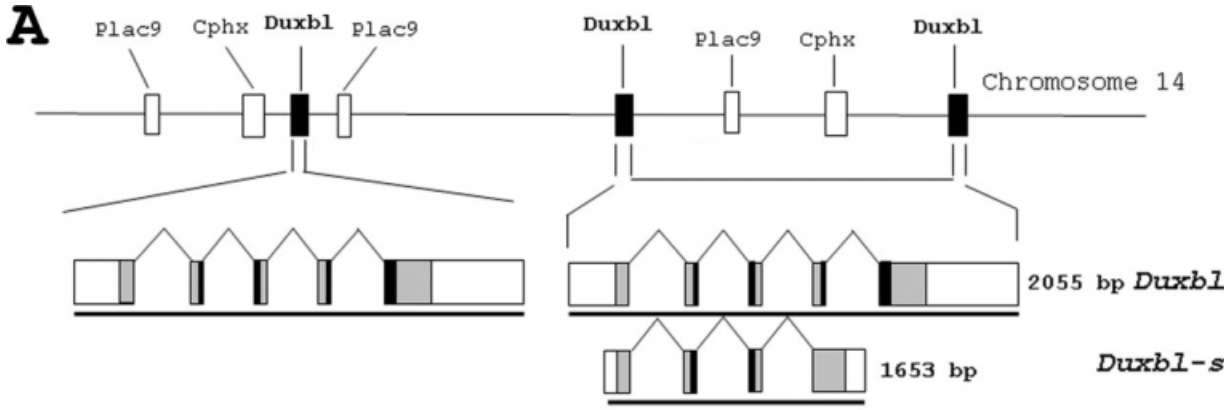

B

```
                                   Homeodomain I (H1)
Duxbl      1 MELSCSTGLLEKEARRRRIILTQSQKDTLRVWFEKNPNPDLATRGHLAKELGISESQIMT  60
Duxbl-s    1 MELSCSTGLLEKEARRRRIILTQSQKDTLRVWFEKNPNPDLATRGHLAKELGISESQIMT  60
                                                  Homeodomain II (H2)
Duxbl     61 WFQKHRKIRKQAEFACCSEESQEQEQDKPRVKEARRSRTHFTKFQTDILIEAFEKNRFPG 120
Duxbl-s   61 WFQKHRKIRKQAEFACCSEESQEQEQDKPRVKEARRSRTHFTKFQTDILIEAFEKNRFPG 120
                              Helix 3                 Helix 1
Duxbl    121 IVTREKLAQQTGIPESRIHIWFQNRRARHPDPGQNTQKTPHPPQSSQGPTQKTVGKLAPS 180
Duxbl-s  121 IVTREKLAQQTGIPESRIHVRCASLCLWQPTCPYHKPLFSRAVDGQSQATHGCPCALDTG 180
               Helix 2
Duxbl    181 KTLTSSASVILPLSPPHTPNGPLDLSKGRQKQLPGTTLLQSSQVVQQRSDDQNPNKGHLS 240
Duxbl-s  181 CKYLVFPATVWRNSHIRPAES*                                       202

Duxbl    241 PTTTPGEQGFHSQPPLQLLTQNRGHNPRESGGLAVPRLEDCTQVPAVNQHFRKLDQNDSS 300
Duxbl-s

Duxbl    301 FLQHWDEWFGSMLAEWMPDKEYWSEKAELHPWQVQLRQLASVSPQAHQTP*          351
Duxbl-s
```

C

```
                          Helix 1          Helix 2          Helix 3          Identity
Duxbl-H1  1 ARRRRIILTQSQKDTLRVWFEKNPNPDLATRGHLAKELGISESQIMTWFQKHRKIRKQAE  60  100% (Mm)
Duxbl-H1  1 --------N-------------------------K---------------------VE  60   93% (Rn)
DUX4-H1   1 G-P--LVW-P--SEA--AC--R--Y-GI---ER--QAI--P-PRVQI---NE-SRQLRQH  60   42% (Hs)
DUXA-H1   1 H--C-TKF-EE-LKI-INT-NQK-Y-GY--KQK--L-INTE--R-QI---NR-ARHGFQK  60   35% (Hs)
DUXA-H1   1 H--C-TKF-EE-LKI-INT-NQK-Y-GY--KQK--L-INTE--R-QI---NR-ARHGFQK  60   35% (Pt)
Rax       1 H--N-TTF-TY-LHE-ERA---SHY--VYS-EE--GKVNLP-VRVQV---NR-AKWRRQE  60   32% (Mm)
Mixl      1 Q--K-TSFSSE-LQL-ELV-RQTMY--IHL-ER--ALTLLP--R-QV---NR-AKSRRQS  60   30% (Mm)
Duxbl-H2  1 ---S-THF-KF-T-I-IWA----RF-GIV--EK--QQT--P--R-HI---NR-ARHPDPG  60   43% (Mm)
                                                    *  *    *

                          Helix 1          Helix 2          Helix 3          Identity
Duxbl-H2  1 ARRSRTHFTKFQTDILIWAFEKNRFPGIVTREKLAQQTGIPESRIHIWFQNRRARHPDPG  60  100% (Mm)
Duxbl-H2  1 -G----------I----E-----------------E----------------------K  60   91% (Rn)
DUX4-H2   1 G--K--AV-GS--AL-LR----D-----AA--E--RE--L-----Q-----------GQ-  60   67% (Hs)
DUXA-H2   1 ---C--TYSAS-LHT--K--M--PY---DS--E--KEI-V----VQ-------S-LLLQR  60   53% (Hs)
DUXA-H2   1 ---C--TYSAS-LHT--K--M--PY---DS--E--KEI-V----VQ-------S-LLLQR  60   53% (Pt)
Rax       1 H--N--T--TY-LHE-ER----SHY-DVYS--E--GKVNL--V-VQV-------KWRRQE  60   45% (Mm)
Mixl      1 Q--K--S-SSE-LQL-ELV-RQTMY-D-HL--R--AL-LL-----QV-------KSRRQS  60   45% (Mm)
```

D

```
                          Helix 1          Helix 2          Helix 3          K + R
Duxbl-H1  1 ARRRRIILTQSQKDTLRVWFEKNPNPDLATRGHLAKELGISESQIMTWFQKHRKIRKQAE  60    8
Duxbl-H2  1 ARRSRTHFTKFQTDILIWAFEKNRFPGIVTREKLAQQTGIPESRIHIWFQNRRARHPDPG  60    6
DUX4-H1   1 GRPRRLVWTPSQSEALRACFERNPYPGIATRERLAQAIGIPEPRVQIWFQNERSRQLRQH  60    6
DUX4-H2   1 GRRKRTAVTGSQTALLLRAFEKDRFPGIAAREELARETGLPESRIQIWFQNRRARHPGQG  60    7
```

Fig. 1. Genomic structure and RNA transcripts of *Duxbl* genes. **A**: The tandem triplicate of mouse *Duxbl* genes and their surrounding genes (*Plac9* and *Cphx*) are present on mouse chromosome 14A3. The lengths of spaces between each *Duxbl* gene and RNA transcripts are indicated. The ORFs of *Duxbl* and *Duxbl-s* transcripts are shown in gray and the regions encoding homeodomains are in black. **B**: Comparison of the predicted amino acid sequences of Duxbl and Duxbl-s proteins. The identical amino acid residues are in bold and the homeodomains are boxed. The different amino acid residues in helix 3 of homeodomain II (H2) are in italics. **C**: Alignment of amino acid sequences of two Duxbl homeodomains (in bold) with those of other predicted homeodomains of double and paired-like homeobox genes. The names of gene products and their homeodomains are listed in the left. Dashes represent sequences identical to those of Duxbl homeodomains. Identity indicates the percentage of sequence identity to Duxbl homeodomain. The asterisks (*) indicate amino acid residues predicted to be involved in sequence-specific DNA binding. **D**: Amino acid sequences of homeodomains of human DUX4 and mouse Duxbl proteins. The basic amino acid residues in two terminal regions of homeodomains are shown in bold. The total numbers of lysine and arginine residues in two ends are shown on the right.

transcript is 2,055 bp in length (Fig. 1A) and was deposited in the NCBI GeneBank, accession number EF472598. Although there are different transcriptional initiation sites found in these *Duxbl* transcripts, they contain the same open reading frame (ORF) of 1,053 bp and a putative polyadenylation signal, AATAAA, at position 2,037 to 2,042. For the two downstream *Duxbl* genes (Gene ID: 72675 and 72672), minor differences in the intron 4 sequences between them and the upstream *Duxbl* gene (Gene ID: 48502) result in producing an additional minor transcript, *Duxbl-s*, composed of four exons (Fig. 1A). More than one transcriptional start sites for *Duxbl-s* transcripts were also identified by 5′ RACE, and they also encode one identical protein. The most abundant *Duxbl-s* transcript is 1,653 bp in length with an ORF of 606 bp, and a putative polyadenylation signal, AATGAA, at position 1,566 to 1,571 (accession number EU257807). The proposed translational start sites for *Duxbl* and *Duxbl-s* transcripts, both correspond to the Kozak consensus site surrounding their start codons (Kozak, 1996). Generations of *Duxbl* and *Duxbl-s* transcripts may result from different promoter usage and/or alternative splicing during development.

Analyzing ORFs of the major *Duxbl* and minor *Duxbl-s* transcripts indicates that the putative Duxbl and Duxbl-s proteins contain 350 and 201 amino acids, respectively (Fig. 1B). The N-terminal 139 amino acid residues of Duxbl and Duxbl-s proteins are identical and contain one domain similar to known homeodomains (homeodomain I, H1). The C terminus of Duxbl protein contains the other homeodomain (homeodomain II, H2); however, Duxbl-s protein does not because it lacks helix 3, the sequence-specific recognition helix (Fig. 1B). Thus, the major product (Duxbl protein) of these three *Duxbl* genes contains two homeodomains, so they are double homeobox genes. Furthermore, the coding regions of all homeodomains for Duxbl and Duxbl-s proteins contain an interrupting intron between homeodomain codon 46 and 47. This is a common feature of *PAXL*-subclass homeodomain proteins (Burglin, 1994). In addition, the amino acid sequences of Duxbl homeodomains share the highest similarities with known *PAXL* homeodomains (Fig. 1C). Therefore, these three *Duxbl* genes belong to *PAXL*-subclass homeobox gene family and they are also mouse double homeobox genes.

Searching for Putative *Duxbl* Ortholog

Although the genomic structure of *Duxbl* is more similar to human *DUXA* gene than human *DUX4* gene, the predicted amino acid sequences of homeodomains for Duxbl and DUX4 proteins are more similar (H1: 42% identity; H2: 67% identity) than those of Duxbl and DUXA proteins (H1: 35% identity; H2: 53% identity; Fig. 1C). Recently, a mouse representative of D4Z4 on chromosome 10 was identified and named as *Dux* (Clapp et al., 2007) and *mDUX* (Bosnakovski et al., 2009), respectively. However, sequence identities of the predicted protein and DUX4 homeodomains (H1: 36% identity; H2: 56% identity) are also lower than those of Duxbl and DUX4. Based on these sequence identities, we suggest that the human ortholog of *Duxbl* gene is *DUX4* gene but not *DUXA* gene as previously reported (Kawazu et al., 2007). Furthermore, comparison of total amino acid sequences of Duxbl protein with those of its predicted ortholog shows that Duxbl protein shares the highest similarity with its rat ortholog (RGD1311053; 80% identity; data not shown). The homeodomain sequences of Duxbl H1 and H2 also exhibit the highest similarity with those of its rat ortholog (93% and 91% identities) followed by its human ortholog (42% and 67% identities; Fig. 1C). Comparisons of homeodomain sequences of Duxbl and other *PAXL*-subclass homeodomain proteins show identities of only 30 to 45% (Fig. 1C). This result indicates that *Duxbl* is a special member of the *PAXL*-subclass homeobox gene family.

Otherwise, the sequence identity between Duxbl H1 and H2 is only 43% (Fig. 1C). We found that Duxbl H1 binds DNA in a nonspecific manner but Duxbl H2 specifically binds a palindromic sequence (Tsai et al., unpublished data). The large differences in amino acid residues and DNA binding properties between Duxbl H1 and H2 suggest that two Duxbl homeodomains may bind and regulate different downstream genes through different mechanisms.

Duxbl Expression Pattern in Adult Tissues

Although many double homeobox genes are found in humans, only DUX4 proteins have been detected in vivo in myoblasts from FSHD patients (Belayew, 2004; Kowaljow et al., 2007). However, the in vivo expression pattern of DUX4 protein is still unknown. Accordingly, we first detected their major and minor transcripts, *Duxbl* and *Duxbl-s*, of these three *Duxbl* genes in various adult tissues by reverse transcriptase-polymerase chain reactions (RT-PCRs). Both *Duxbl* and *Duxbl-s* transcripts are predominantly expressed in adult eye, brain, and reproductive organs including ovary, uterus, placenta and testis (Fig. 2A). We next performed Western blotting to decipher in vivo expressions of Duxbl proteins in adult mouse tissues using affinity-purified homemade Duxbl polyclonal antibodies. A 38-kDa protein band indicating Duxbl protein is predominantly detected in adult eye, brain and ovary (Fig. 2B). The results of *Duxbl* expression patterns in adult tissues by RT-PCRs (Fig. 2A) and Western blotting (Fig. 2B) are complementary, because we only detected Duxbl proteins in adult tissues with strong *Duxbl* transcript signals. However, Duxbl-s protein is not detected in these adult tissues by our polyclonal antibodies. This may result from the much lower expression levels of *Duxbl-s* transcripts than *Duxbl* transcripts in these tissues (Fig. 2A).

Blocking assays for preincubations of polyclonal antibodies with purified glutathione S-transferase (GST) proteins or GST-H1 and GST-H2 fusion proteins were used to verify the specificity and activity of our Duxbl polyclonal antibodies. After preincubation with GST-H1 and GST-H2 fusion proteins, the purified Duxbl polyclonal antibodies did not recognize the previously identified Duxbl proteins in adult ovary and overexpressed Duxbl-V5 fusion proteins (Fig. 2C). However, antibodies preincubated with GST proteins could recognize Duxbl proteins in adult ovary, overexpressed Duxbl-V5 fusion proteins, and purified 6His-Duxbl fusion proteins. This result verifies the activity and specificity of our

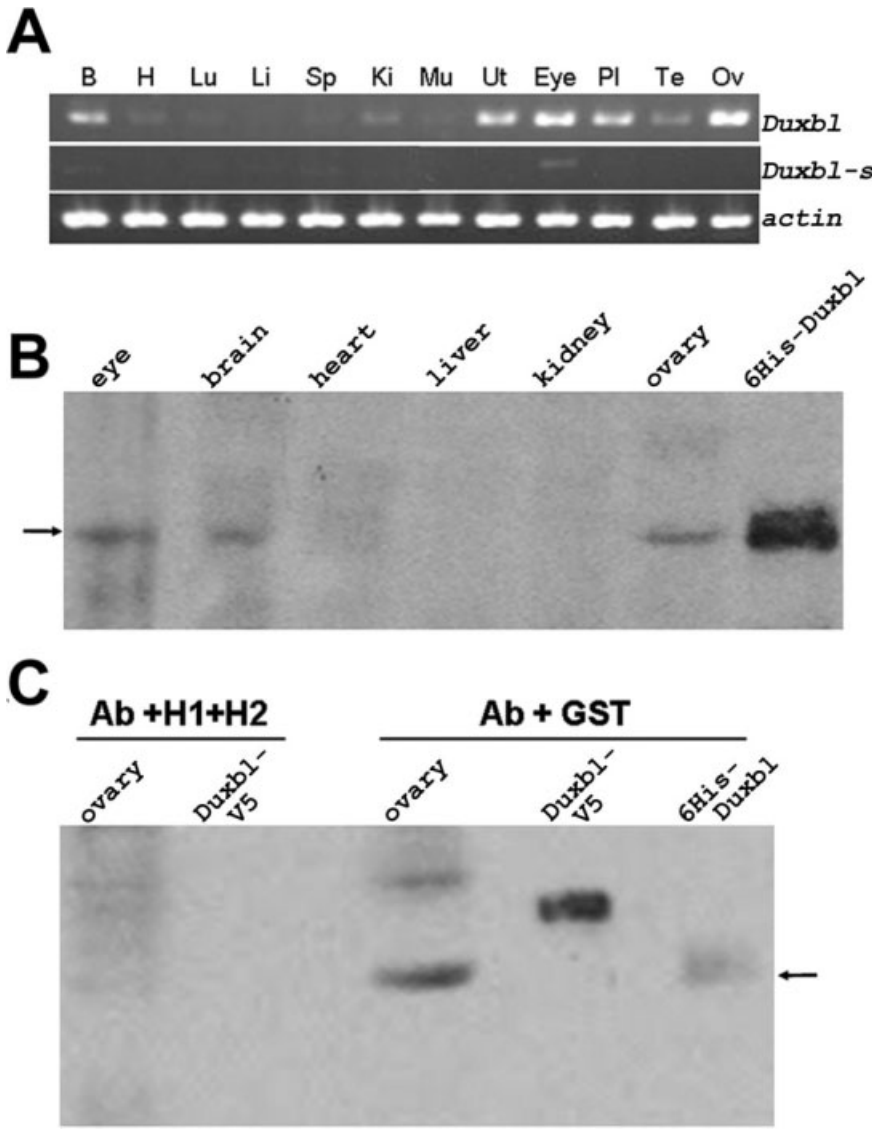

Fig. 2. Expression profiles of *Duxbl* and *Duxbl-s* transcripts and Duxbl protein. **A**: The expression levels of *Duxbl* and *Duxbl-s* transcripts in adult mouse tissues were analyzed by reverse transcriptase-polymerase chain reactions (RT-PCRs). Expression level of *actin* was used as an internal control. B, brain; H, heart; Lu, lung; Li, liver; Sp, spleen; Ki, kidney; Mu, skeletal muscles; Ut, uterus; Eye, eye; Pl, placenta; Te, testis; Ov, ovary. **B**: Purified Duxbl fusion protein containing N-terminal 6 histidine residues (6His-Duxbl) and equal-amount of total proteins extracted from indicated adult tissues were analyzed by Western blotting using affinity-purified Duxbl polyclonal antibodies. **C**: Analyzing the specificity of purified Duxbl polyclonal antibodies. The purified Duxbl polyclonal antibodies were preincubated with purified GST-H1 and GST-H2 fusion proteins (Ab +H1+H2) or with GST proteins only (Ab +GST). Total proteins extracted from adult ovaries and HeLa cells transfected with Duxbl-V5 fusion protein expression vectors (Duxbl-V5), or purified 6His-Duxbl fusion proteins were analyzed by Western blotting using two different pretreated antibodies. Position of 38-kDa protein bands representing Duxbl proteins was indicated by arrow.

homemade affinity-purified Duxbl polyclonal antibodies.

Duxbl Expression Patterns in Gonads

Because *Duxbl* is predominantly expressed in adult ovary and slightly expressed in adult testis (Fig. 2A), we examined *Duxbl* expression levels in embryonic and postnatal gonads by RT-PCRs. In female gonads, *Duxbl* transcripts are observed from embryonic day 12.5 (E12.5) until birth (Fig. 3A). After birth, *Duxbl* expressions in the ovaries are found to be high until adulthood. In male gonads, *Duxbl* transcripts are also detected from E12.5 until birth (Fig. 3B). After birth, *Duxbl* expressions peaked at day 7 and returned to low levels from day 21 until adulthood. Furthermore, the expression patterns of *Duxbl-s* transcripts are similar to but lower than those of *Duxbl* transcripts (Fig. 3A,B). In addition, low levels of *Duxbl* transcripts are also detected in the mesonephros (data not shown). Because no *Duxbl* expression is detected in mouse Leydig (TM3), Sertoli (TM4), and spermatocyte (GC-2) cell lines (data not shown), we suggest that *Duxbl* expresses in germ cells. To verify this suggestion, we performed quantitative RT-PCRs in male gonads. Results of real-time RT-PCRs confirm the increases of *Duxbl* expressions after birth. *Duxbl* expressions in male testes peak at day 7 (Fig. 3C), while male gonocytes exit cell cycle arrest and enter a wave of spermatogonia proliferation. *Duxbl* expressions were seen decreasing from day 15 to adulthood. Before birth, there is a *Duxbl* expression peak with a moderate expression level observed around E13.5, a time for rapid proliferations of male germ cells. After this time, the proliferations of male germ cells slow down and enter mitotic arrest at around E16.5 (Olaso and Habert, 2000). Results of quantitative RT-PCRs suggest high *Duxbl* expressions in proliferating male germ cells including gonocytes and spermatogonia.

We further characterized *Duxbl* expressions in adult testis by in situ hybridizations to decipher the cellular localizations of *Duxbl* transcripts. In adult testis sections, strong *Duxbl* transcript signals are only detected in spermatogonia from stage X to XII seminiferous tubules (Fig. 4A). However, we did not detect any *Duxbl* signal in postmeiotic cells of testis including spermatocytes and spermatids. The *Duxbl* expressions in spermatogonia and the absence in other postmeiotic cells are also confirmed by RT-PCRs of germ cells isolated from distinctive stages (data not shown). Results of in situ hybridizations in adult testis (Fig. 4A) are identical to results of RT-PCRs from testis cell lines, because we could not detect *Duxbl* expression in Leydig and Sertoli cells, and in round spermatids (data not shown). Pang and his coworkers also identified differential expressions of 1110051B16Rik gene in

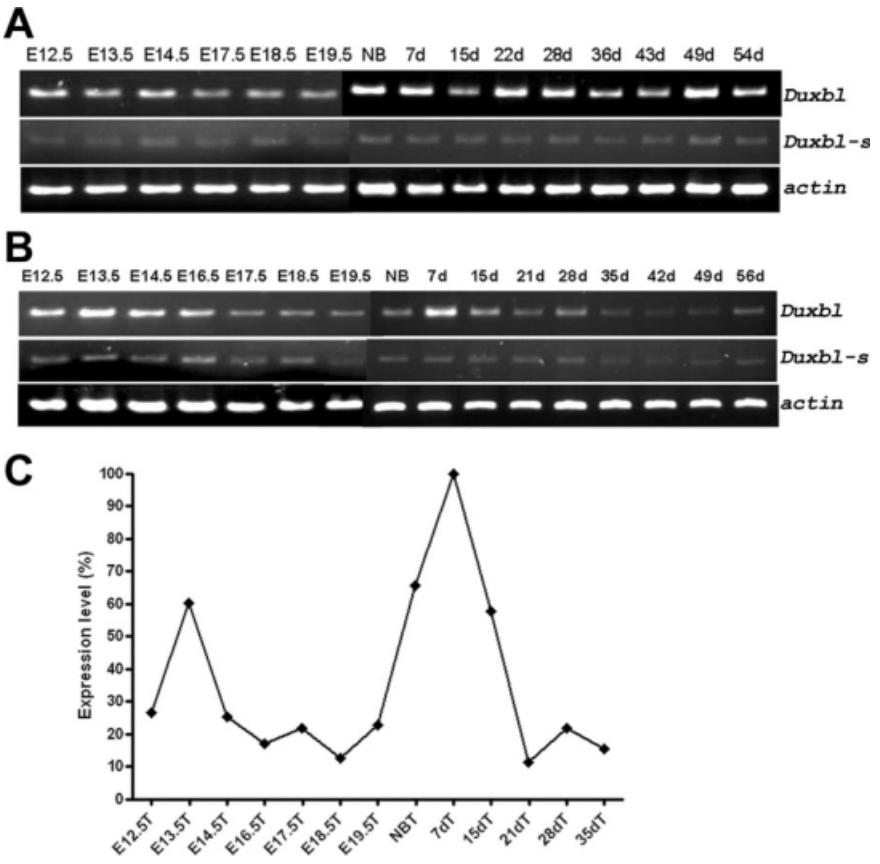

Fig. 3. Analyses of expression levels and profiles of *Duxbl* and *Duxbl-s* transcripts during gonad developments. **A,B**: The expression levels of *Duxbl* and *Duxbl-s* transcripts in female (A) and male (B) gonad developments were analyzed by reverse transcriptase-polymerase chain reactions (RT-PCRs). Total RNAs were extracted from ovaries (A) or testes (B) from different embryonic days (E12.5 to E19.5), newborn mice (NB), and mice at different postnatal days (7d to 56d). Expression levels of *actin* were used as internal controls. **C**: Analysis of *Duxbl* expression levels in testes by real-time RT-PCRs. The relative expression levels of *Duxbl* to *GADPH* transcripts in testes from different embryonic and postnatal days were determined. The relative expression levels were shown after comparison with the expression level of 7-day-old testes.

spermatogonia by microarray and quantitative RT-PCR at different stages of spermatogenesis (Pang et al., 2003). Furthermore, we performed in situ hybridizations to find cells that specifically express *Duxbl* in adult ovary. In adult ovary sections, weak expressions of *Duxbl* transcripts are found in the oocytes of primordial follicles, but strong expressions are seen in the oocytes of primary and secondary follicles (Fig. 4B). These results indicate that *Duxbl* are specifically expressed in oocytes during oogenesis and in spermatogonia during spermatogenesis.

We next examined the in vivo localizations of Duxbl proteins in 2-week-old and adult ovaries by immunohistochemistry using homemade affinity-purified Duxbl polyclonal antibodies. Results of immunostained ovary sections show that Duxbl proteins are specifically present in oocytes of primordial, primary, secondary, and antral follicles (Fig. 5). These results of in vivo Duxbl protein localizations are consistent with results of in situ hybridizations (Fig. 4B), because we obtain oocyte-specific signals of *Duxbl* transcripts and Duxbl proteins in the same types of follicles in both cases.

Subcellular Localizations of Duxbl and Duxbl-s Proteins

We used the same homemade Duxbl polyclonal antibodies to examine the subcellular localizations of overexpressed epitope-tagged Duxbl and Duxbl-s proteins, respectively. Results of immunofluorescence reveal that the overexpressed Duxbl-V5 and FLAG-Duxbl-s fusion proteins are both restricted to the nuclei of transfected cells (Fig. 6). We observed the same subcellular localizations of Duxbl and Duxbl-s fusion proteins using commercial anti-V5 and anti-FLAG monoclonal antibodies, respectively (data not shown). These results indicate that both overexpressed Duxbl and Duxbl-s proteins contain the nuclear localization signal (NLS). Although the amino acid residues of homeodomains from various homeodomain proteins show a high degree of conservation, NLSs of homeodomain proteins are not identical. A common theme of their NLSs is the basic amino acid residues at two ends of homeodomains (Ploski et al., 2004; Ostlund et al., 2005). The first (H1) and the second (H2) homeodomains of Duxbl protein contain 8 and 6 lysine/arginine residues at their two ends, respectively (Fig. 1D). In addition, the human DUX4 protein also contains 6 and 7 lysine/arginine residues at two ends of its H1 and H2, respectively (Fig. 1D). Previously, DUX4 protein has been shown to transactivate *PITX1* expression (Dixit et al., 2007). Because Duxbl and Duxbl-s proteins contain similar lengths of basic residues as DUX4 protein at two ends of their homeodomains (Fig. 1D) and both of them localize in the nuclei (Fig. 6), they might transactivate downstream gene(s) as DUX4 protein. However, overexpressing Duxbl proteins in C2C12 cells could not transactivate *Pitx1* expression (data not shown).

Duxbl Expression Patterns in Embryonic Development

Because *Duxbl* transcripts are predominantly restricted in oocytes of ovary (Fig. 4B), *Duxbl* expressions during embryonic development were further determined. *Duxbl* transcripts are first detected in unfertilized eggs then continued to blastocysts but not in cumulus cells (Fig. 7A). After implantation, *Duxbl* expressions in embryos are seen decreased from embryonic day 11.5 (E11.5) to 17.5 (E17.5), and *Duxbl-s* shows similar expression pattern (Fig. 7B). Furthermore, whole-mount in situ hybridizations were used to identify *Duxbl* transcripts in developing mouse embryos from E9.5 to E12.5. The *Duxbl* transcripts are detected in forelimb, hindlimb, and tail beginning from E9.5 and maintained to E12.5 (Fig. 7C–E). *Duxbl* expressions in limbs were

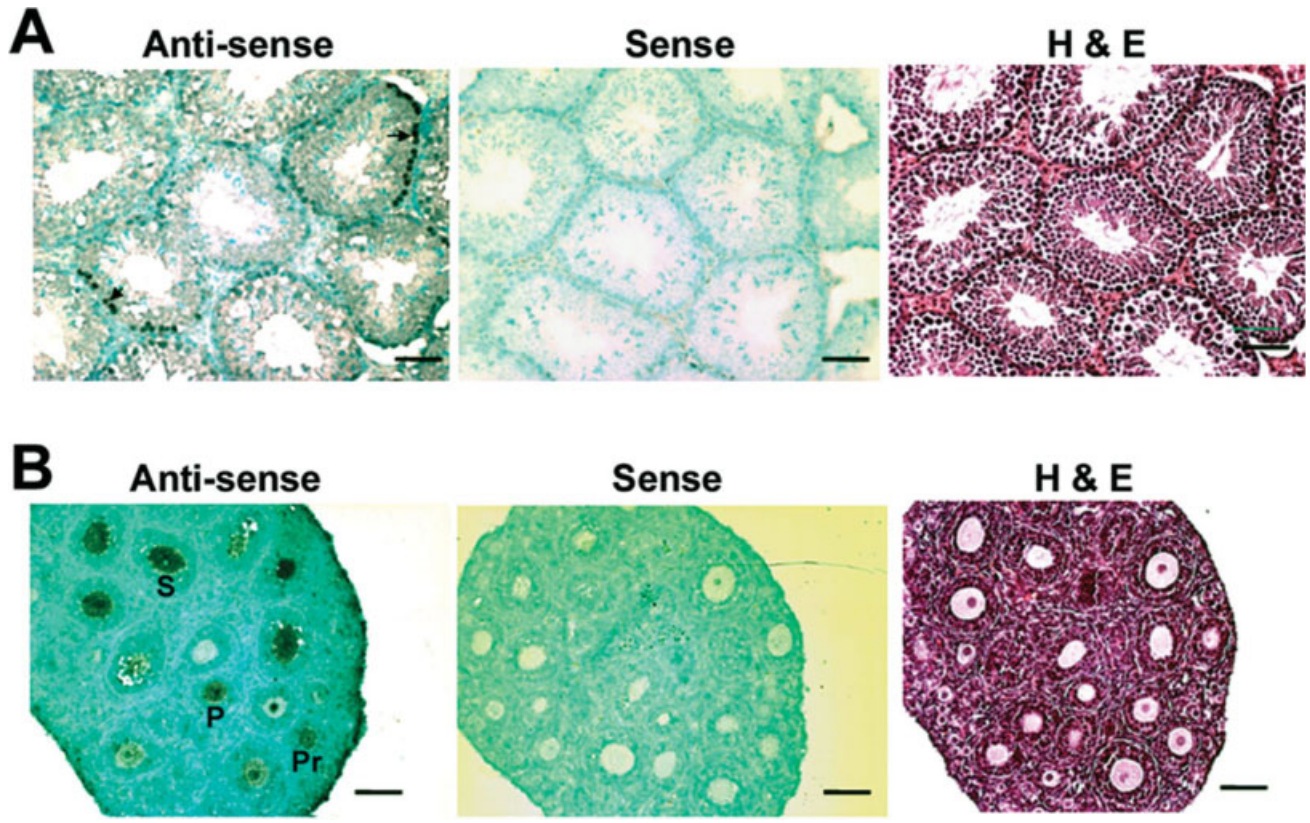

Fig. 4. Identifying *Duxbl* transcripts in gonads by in situ hybridizations. **A,B**: The localizations of *Duxbl* transcripts were analyzed in adult testis (A) and 10-day-old ovary (B). Adjacent sections were labeled with digoxigenin-labeled anti-sense (left panel) and sense probes (middle panel), or stained with hematoxylin and eosin (H&E, right panel). *Duxbl* transcripts were only detected in spermatogonia (indicated by arrows) of testis (A) and in oocyte of primordial (Pr), primary (P), and secondary (S) follicles in ovary (B). Scale bars = 50 μm.

further detected by section in situ hybridization and Alcian blue staining. *Duxbl* signals are localized in muscle cells (data not shown). Furthermore, in vivo Duxbl protein expressions were analyzed by immunohistochemistry. Strong Duxbl protein signals are detected in muscle cells of limbs at E13.5 embryo (Fig. 7F), while myotubes begin to form. Especially, Duxbl protein signals are detected in the fiber-like muscle cells but not in the mononuclear cells expressing MyoD proteins (Fig. 7G). These results indicate that Duxbl proteins are expressed in limbs and tail during embryo development and in differentiated myocytes but not in myoblasts.

Duxbl Expressions During Limb Development

During muscle development in limbs, muscle progenitor cells from somite migrate into limb bud, where they proliferate, express myogenic determination factors and subsequently

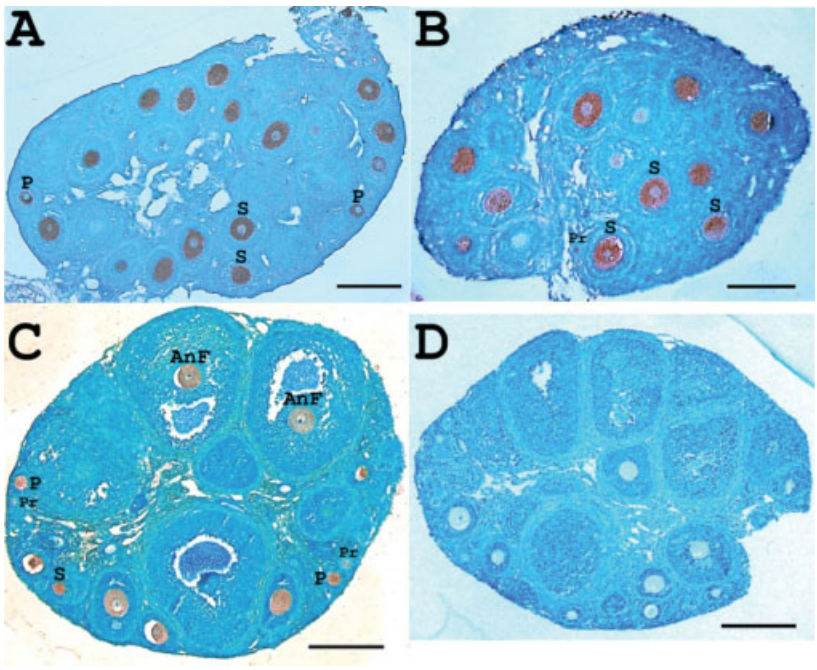

Fig. 5. Identifying Duxbl proteins in 2-week-old and adult ovaries by immunohistochemical analysis. **A–D**: Duxbl proteins in 2-week-old (A,B) and adult (C,D) mouse ovary sections were probed using affinity-purified Duxbl polyclonal antibodies (A–C) and normal rabbit immunoglobulin G (D), respectively. Duxbl proteins are specifically present in oocytes of primordial (Pr), primary (P), secondary (S), and antral follicles (AnF) as indicated. Scale bars = 50 μm.

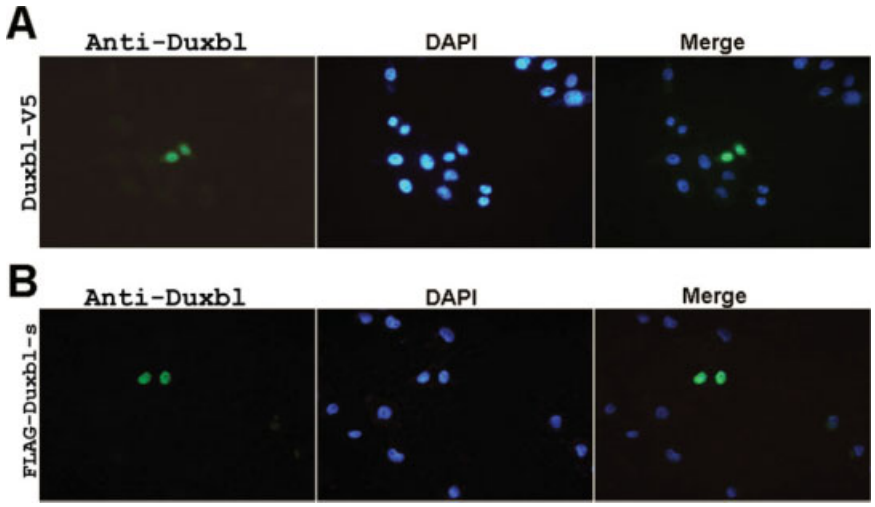

Fig. 6. **A,B**: Subcellular localizations of overexpressed Duxbl and Duxbl-s proteins. Duxbl-V5 (A) and FLAG-Duxbl-s (B) fusion proteins were overexpressed in HeLa cells by transfection of Duxbl-V5 and FLAG-Duxbl-s expression vectors, respectively. The overexpressed Duxbl-V5 or FLAG-Duxbl-s proteins were detected by affinity-purified anti-Duxbl polyclonal antibodies (left panel). Cell nuclei were stained with DAPI (middle panel). Images of left and middle panels were merged (right panel).

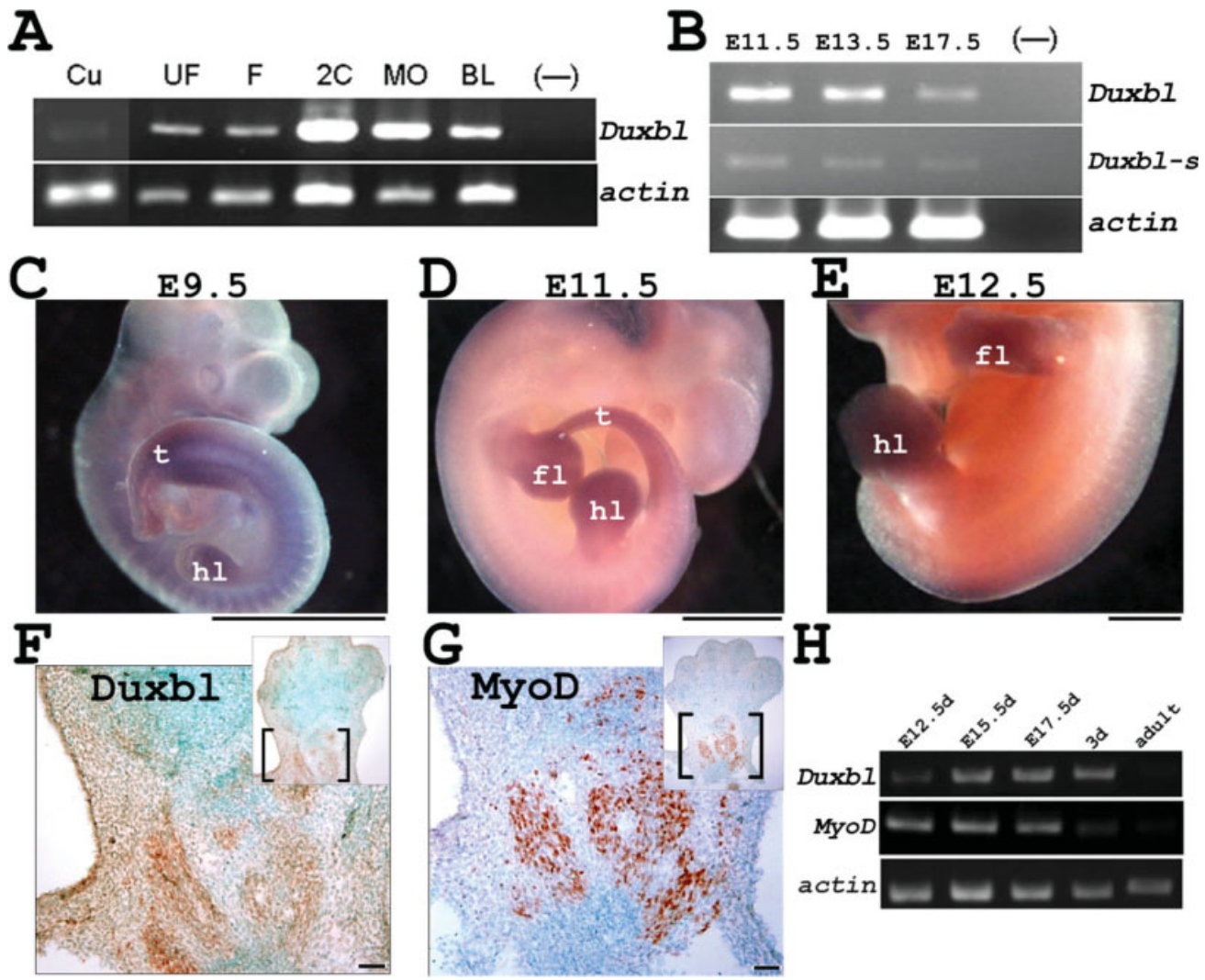

Fig. 7. Identifying *Duxbl* expressions during mouse development by reverse transcriptase-polymerase chain reaction (RT-PCR), whole mount in situ hybridization, and immunohistochemical analysis. **A,B**: Expressions of *Duxbl* and *Duxbl-s* transcripts in preimplantation (A) and postimplantation (B) embryos were analyzed by RT-PCRs. A: Cu, cumulus cells; UF, unfertilized eggs; F, fertilized eggs; 2C, two-cell embryos; MO, morula; BL, blastocysts. B: Total RNAs were extracted from postimplantation embryos at embryonic day 11.5 (E11.5), 13.5 (E13.5), and 17.5 (E17.5), respectively. Amplifications without RNA served as negative controls (−). **C–E**: Identifying *Duxbl* expressions in different embryos at embryonic day 9.5 (E9.5), 11.5 (E11.5), and 12.5 (E12.5) by whole-mount in situ hybridizations, respectively. t: tail; fl: forelimb; hl: hindlimb. **F,G**: Identifying Duxbl and MyoD protein expressions in dorsal sections through forelimb of 13.5-day embryo by immunohistochemical analysis using anti-Duxbl (F) and anti-MyoD (G) antibodies, respectively. The boxed regions in small figures were amplified. **H**: Analyzing *Duxbl* and *MyoD* expression levels by RT-PCRs during embryonic and postnatal limb developments. Total RNAs were extracted from limbs at embryonic day 12.5 (E12.5), 15.5 (E15.5), and 17.5 (E17.5), and at postnatal day 3 (3d) and adult, respectively. Expression levels of *actin* were used as internal controls. Scale bars = 50 μm.

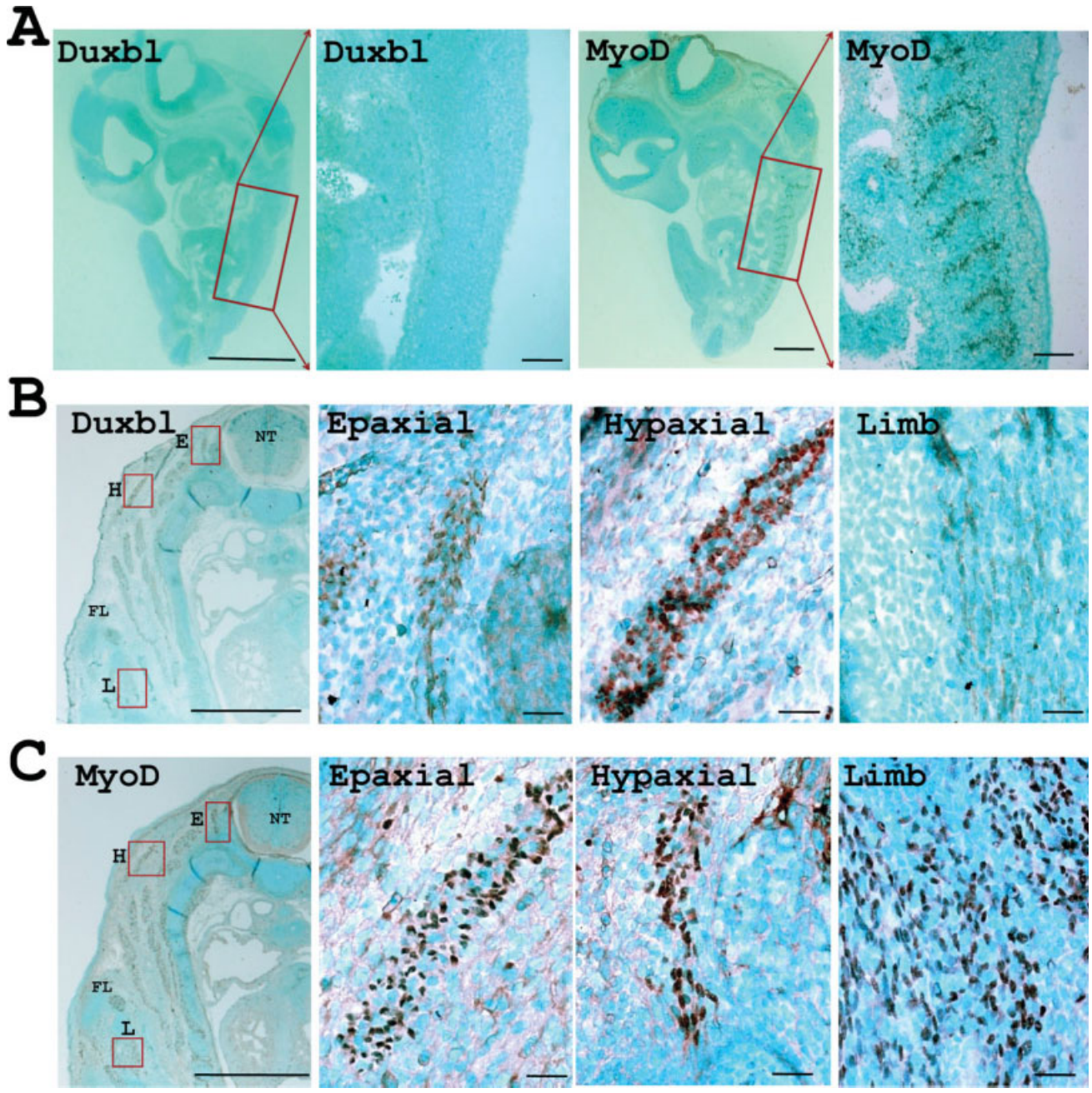

Fig. 8. Identifying Duxbl and MyoD protein expressions in embryonic muscles. A–C: Duxbl and MyoD proteins were detected on parasagittal sections of 11.5-day embryo (A) and transverse sections of 12.5-day embryo (B,C) by immunohistochemistry. **A**: High magnifications of the boxed regions in the left panels were shown in the right. **B,C**: High magnification of the boxed regions in the left panels of epaxial (E), hypaxial (H), and limb (L) muscles were shown in the middle and right panels as indicated. FL, forelimb; NT, neural tube. Scale bars = 50 μm.

differentiate into skeletal muscles. MyoD and myogenin (MyoG) are first detected in the proximal regions of both hindlimb and forelimb at embryonic day (E) 11.5 embryo and later accumulated in the differentiated muscle masses, continuously expressed in fetal skeletal muscles (Sassoon et al., 1989). Although expressions of *Duxbl* and *MyoD* are both continuous from E12.5 to postnatal stage (3d) in limbs by RT-PCR analyses (Fig. 7H), *Duxbl* expressions in limbs are largely increased from E12.5 to E15.5 and maintained in high level to postnatal (3d) stage, but almost undetectable in adult muscles by RT-PCR analyses (Fig. 7H). These results suggest that *Duxbl* expressions are low in myoblast proliferation stage but increase largely following myotube formation, so Duxbl may play a role in myogenesis during embryonic limb development.

Duxbl Protein Expressions in Trunk Myogenesis

During embryogenesis, skeletal muscles in the trunk and limbs are both derived from somites (Tajbakhsh and

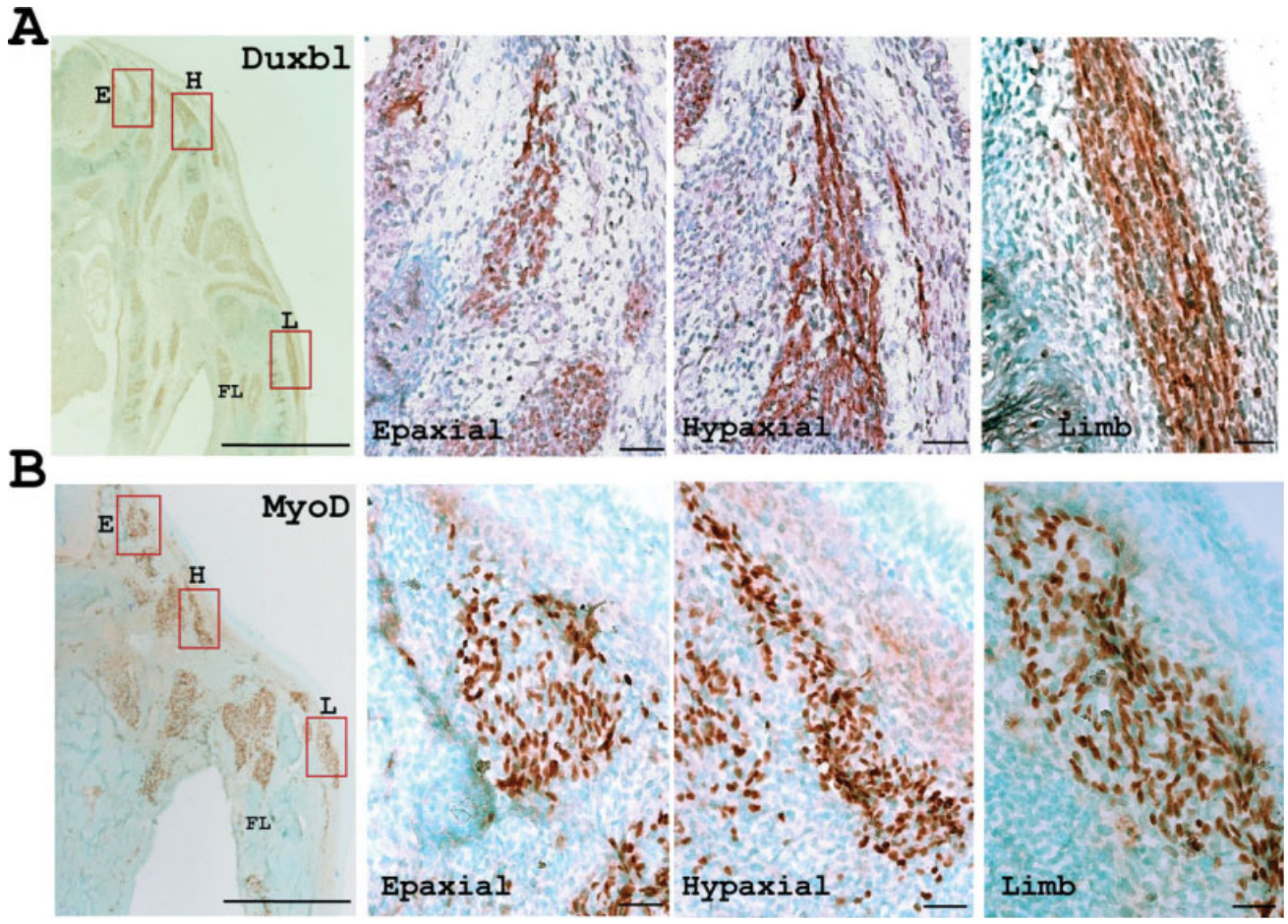

Fig. 9. Identifying Duxbl and MyoD protein expressions in developing muscles. Duxbl (A) and MyoD (B) proteins were detected on transverse sections of 13.5-day embryo by immunohistochemistry. **A,B**: High magnification of the boxed regions in the left panels of epaxial (E), hypaxial (H), and limb (L) muscles were shown in the middle and right panels as indicated. FL, forelimb. Scale bars = 50 μm.

Buckingham, 2000). During myotome development, MyoG and MyoD are detectable at E10.5 (Cusella-De Angelis et al., 1992), while terminally differentiated muscle cells could already be identified in the myotome. To decipher the Duxbl protein expressions during myotome development in advance, we used immunohistochemistry on parasagittal sections of E11.5 embryos. Duxbl protein is not detected in somite (Fig. 8A). However, the myoblast marker gene products, MyoD proteins, are expressed in the myotomes. To further confirm the expressions of Duxbl proteins during skeletal myogenesis in the trunk and limb, we used immunohistochemistry on transverse sections of embryo at E11.5 with antibodies react with MyoD and Duxbl proteins, respectively. In transverse sections of the same embryo, MyoD-positive cells are also observed in myoblasts of developing limbs and somite. However, no Duxbl-expressing cells are present in transverse sections of the same E11.5 embryos (data not shown). In further embryonic development, Duxbl is seen expressed in the epaxial, hypaxial, and forelimb muscles in E12.5 embryo (Fig. 8B), similar to MyoD (Fig. 8C). However, the intensities of Duxbl proteins are less than MyoD proteins in all muscle-forming regions, especially in limb muscles. After comparing stained cell morphology, Duxbl proteins are obviously stained in fewer elongated myocytes and immature myofibrils (Fig. 8B). However, MyoD proteins are detected in mononuclear myocytes (Fig. 8C). These results suggest that Duxbl expressions are low in limb myoblast proliferation stage, embryonic day 12.5. After myoblast proliferation stage, at E13.5 embryo, myoblasts have clearly acquired a spindle-shaped morphology, and considerably more and longer myofibrils have now been formed. In E13.5 embryonic transverse sections, Duxbl proteins are expressed in increased number of cells, virtually including all of the newly formed primary fibers, present in both body wall and limbs (Fig. 9A). Strong Duxbl signals are detected in elongated myocytes and multinuclear myotubes (Fig. 9A). The distribution and intensity of Duxbl expressions are both similar to those of myosin heavy chain (MHC; Kablar et al., 1997). MHC is expressed exclusively in terminally differentiated myotubes and is detectable in the intercostal muscles of the trunk and the muscle anlagen of forelimb. The expressions of both Duxbl and MHC are increased in E13.5 embryo, in which stage the myotube formations are observed.

Duxbl Expressions During C2C12 Cell Differentiation

To verify that *Duxbl* is expressed in differentiated myocytes but not in

myoblasts during skeletal muscle formation, we examined *Duxbl* expressions during in vitro differentiations of C2C12 cells. *Duxbl* transcripts are slightly detected in confluent myocytes, and seen significantly increased in differentiated cells following 2 days in differentiation medium as *MyoG* (Fig. 10A). Because *Duxbl* exhibits similar expression patterns as *MyoG* during C2C12 cell differentiation, we suggest that Duxbl also play a role in myoblast differentiation and/or fusion. Our double immunofluorescence data also show the presence of Duxbl protein signals in differentiating cells and clearly located in the nuclei of multinuclear myotubes (Fig. 10B), similar to results of in vivo immunohistochemistry analyses (Figs. 7F, 8B, 9A). However, MyoD proteins are stained strongly in small nuclear myoblasts and myocytes, while only slightly in myotubes (Fig. 10B). From the above results, we conclude that Duxbl is expressed in myotubes but not in proliferating myoblasts during in vitro differentiation of myoblasts and in vivo skeletal muscle formation. Because the expression of *Duxbl* is downstream of *MyoD* and seems parallel to *MyoG*, whether expression of Duxbl influences *MyoD* or *MyoG* or other muscle specific genes to affect myogenesis need further characterizations. C2C12 can be used as a model cell line to identify the molecular mechanism of Duxbl influencing myoblast differentiation or how Duxbl interact with the myogenic regulatory factors to regulate myogenesis.

In brief, *Duxbl* is a mouse double homeobox gene that contains introns. The Duxbl homeodomain exhibits the maximum identities to those of human DUX4 gene. From the homeodomain similarity, we suggest that *Duxbl* is the ortholog of human *DUX4*, which is the candidate gene to cause FSHD. However, the exact expression pattern of DUX4 in human development or during myogenesis is not detected and might be undetectable, because DUX4 protein cannot be obtained from normal adult tissues. Studying the expression profile of a mouse double homeobox gene, *Duxbl*, can facilitate the understanding of the functions of double homeobox genes including *DUX4* during development. In addition, the characterization of Duxbl expression during myogenesis might help in understanding the molecular mechanism of FSHD. During

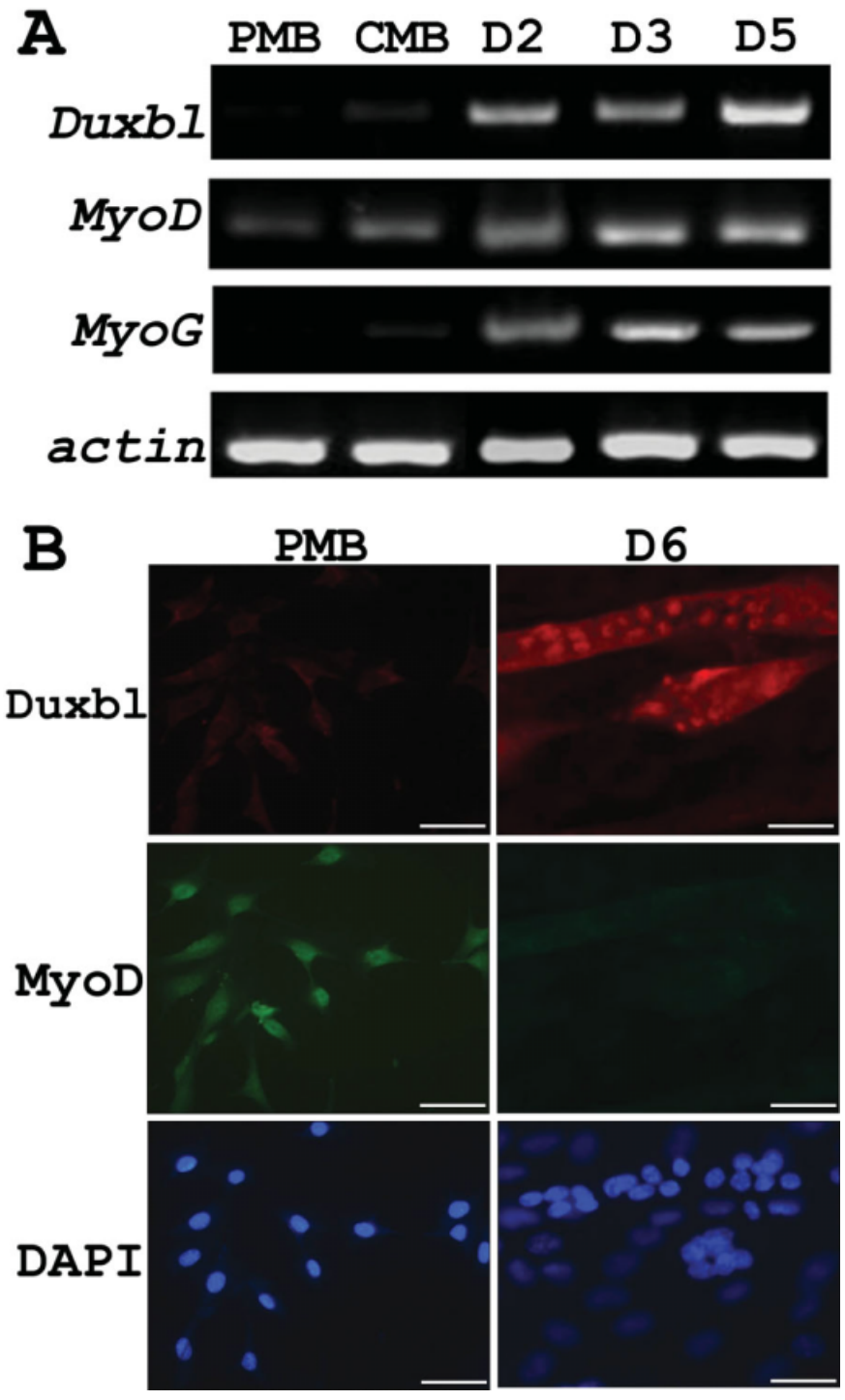

Fig. 10. Identifying *Duxbl*, *MyoD*, and *MyoG* expressions in differentiated and undifferentiated C2C12 cells. **A**: Expression levels of *Duxbl*, *MyoD*, and *MyoG* transcripts were determined by reverse transcriptase-polymerase chain reactions (RT-PCRs) during C2C12 differentiation. Total RNAs were extracted from proliferating myoblasts (PMB), confluence myoblasts (CMB), and differentiating myocytes cultured in differentiation medium for 2, 3, and 5 days (D2, D3, D5), respectively. Expression levels of *actin* were used as internal controls. **B**: Double immunofluorescence analysis of Duxbl and MyoD expressions in C2C12 cells. C2C12 cells were incubated in growth medium as proliferating myoblasts (PMB) and in differentiation medium for 6 days (D6) as differentiating myocytes, respectively. They were analyzed by double immunofluorescence with anti-Duxbl and anti-MyoD antibodies. Signals of Duxbl proteins were detected with Texas red-conjugated secondary antibodies (Duxbl) and signals of MyoD were detected with fluorescein isothiocyanate (FITC) -conjugated secondary antibodies (MyoD). Cell nuclei were stained with 4′-6-diamidino-2-phenylindole (DAPI). Scale bars = 50 μm.

embryo development, Duxbl is predominantly expressed in differentiated myocytes during embryo skeletal myogenesis. The myofibers of epaxial, hypaxial, and limb express Duxbl proteins, first, from E12 embryo. However, Duxbl is barely detectable in the adult limb muscle. Because DUX4 protein can be detected in primary myoblasts extracted from FSHD patients but not from normal people, we suggest that an increase in the expression of embryo protein, mDux in adult tissue may develop a muscular dystrophy with features characteristic of the human disease. In addition to skeletal myogenesis, Duxbl is also expressed in germ cells, especially in oocytes and spermatogonia, during gonad development. Our results suggest that Duxbl is important in germ cell development. Our future experiments would be directed toward characterizing the exact function of this gene using transgenic or conditional knockout analysis.

EXPERIMENTAL PROCEDURES

Animals

Mice were maintained in a specific pathogen-free environment at the animal housing in Chung Shan Medical University. All experimental procedures were conducted in accordance with the guidelines of the institutional animal committee and received protocol number 401.

RNA Isolations and RT-PCRs

Total RNAs were extracted using Trizol reagent (Life Technologies) from various mouse tissues, embryos at different stages, and various mouse cell lines. Quantities and purities of RNAs were determined by ultraviolet absorbance (DU 800; Beckman Coulter) and by gel electrophoresis. Five or two micrograms each of total RNAs were reverse transcribed using Superscript II system (Life Technologies) and oligo-dT primer. P1/GSP1 (P1, 5′-GAGCTGCAGTACTGGCCTACTG-3′; GSP1, 5′-CTGGGAGGACTGAAGTAGTGTGGT-3′) and P1/GSP2 (GSP2, 5′-ATGATTATGCAGGTCTGATGTG-3′) primer pairs were used to determine the expressions of *Duxbl* and *Duxbl-s* transcripts (Fig. 1A), respectively. As positive controls, the expression of β-*actin* gene was detected using the following primers: Actin F: 5′-GAGACCTTCAACACCCCAGC-3′ and Actin R: 5′-AGGAAGGCTGGAAAAGAGCC-3′.

Cloning the Full-Length cDNAs

Because *Duxbl* and *Duxbl-s* transcripts are predominantly expressed in adult ovary, total ovary RNAs were used to characterize the full-length *Duxbl* and *Duxbl-s* transcripts. The 5′ and 3′ end sequences of *Duxbl* and *Duxbl-s* transcripts were obtained by 5′ and 3′ RACE-PCRs using the SMART RACE cDNA amplification kit (Clontech), respectively. Total RNAs were reversely transcribed using 5′ or 3′ CDS primers. The resultant cDNA products were subjected to PCR for generating the 5′ and 3′ *Duxbl* and *Duxbl-s* cDNA fragments, respectively, using transcript-specific primers (GSP1, GSP2, or GSP3: 5′-AGCAGGAGCAGGATAAACCTAGAGTTAAAGA-3′) and UPM primer. The PCR products were then subjected to nested PCR using transcript-specific primers (GSP1 or GSP2) and nested universal primer A. Finally, the PCR products were analyzed on 1.2% agarose gels, subcloned into pGEM-T Easy vectors (Promega) and then sequenced.

Real-Time PCRs

Total RNAs were extracted from testes at different stages using TRI Reagent (Sigma-Aldrich). Primers for real-time PCRs were designed for mouse *Duxbl* and *GAPDH* transcripts. The forward primer for *Duxbl* was 5′-GCATCTCTGAGTCTCAAATTATGACTTG-3′, and the reverse primer was 5′-GCGTTCTGCTCCTTCTAGCTTCT-3′. The forward primer for *GAPDH* was 5′-TGTGTCCGTCGTGGATCTGA-3′, and the reverse primer was 5′-CCTGCTTCACCACCTTCTTG-3′. Complementary DNAs were synthesized from RNA samples using Superscript II RNase H-minus reverse transcriptase (Invitrogen) according to the manufacturer's protocol, and then cDNAs were used as templates for real-time PCR assays using the ABI Prism 7000 Sequence Detection System (Applied Biosystems). Threshold (Ct) values for *Duxbl* and *GADPH* transcripts were determined using Prism SDS software version 1.0 (Applied Biosystems).

Expressions and Purifications of Duxbl Homeodomain Fusion Proteins

The coding regions of Duxbl N-terminal homeodomain (H1) and C-terminal homeodomain (H2) were PCR amplified, gel-purified, and then subcloned into pGEX-6P-2 expression vectors (Amersham). After induction, the expressed glutathione-S-transferase (GST) fusion proteins, GST-H1 and GST-H2, were purified using Glutathione Sepharose beads (Amersham). The forward primer for H1 homeodomain was 5′-CGGAATTCTTGAGCTGAGCTGCAGT-3′, and the reverse primer was 5′-CCCTCGAGCTATGCAAACTCTGCTTG-3′. The forward primer for H2 homeodomain was 5′-CGGAATTCTTAGAGTTAAAGAAGCTAGAAG-3′, and the reverse primer was 5′-GCGGCC-GCTTAAGTTTTCTGAGTGTTCTGTCC-3′.

Production of Anti-Duxbl Polyclonal Antibodies and Western blotting

The *Duxbl* coding region was PCR amplified, gel-purified, and then inserted into the pAE expression vector (Ramos et al., 2004). The Duxbl fusion proteins containing 6 histidine residues at the N-terminus (6His-Duxbl) were overexpressed and then purified using His-bind resin (Novagen), before being used to immunize rabbits for generation of anti-serum against Duxbl proteins. These anti-Duxbl polyclonal antibodies were purified by affinity chromatography using 6His-Duxbl fusion proteins. To test the immunospecificity of purified anti-Duxbl antibodies, we performed a blocking assay using antibodies pretreated with purified GST-H1 and GST-H2 proteins or GST protein only. To detect Duxbl protein in various mouse tissues, equal amount of total proteins extracted from various adult mouse tissues were separated in 12% sodium dodecyl sulfate-polyacrylamide gels and electro-transferred onto polyvinylidene fluoride membranes (Millipore). Expression levels of Duxbl proteins were then determined by Western blotting using purified anti-Duxbl polyclonal antibodies.

Whole-Mount In Situ and Section In Situ Hybridizations

Expressions of the *Duxbl* gene were analyzed by in situ hybridizations using a 660-bp *Duxbl* cDNA fragment (265-925), which encodes the coding region of Duxbl protein. The 660-bp *Duxbl* cDNA fragments (position 265-925) were subcloned into pGEM-T Easy vectors. The sense and anti-sense riboprobes were prepared by in vitro transcriptions using SP6 and T7 RNA polymerases with digoxigenin (Dig)-UTP (Boehringer Mannheim), respectively. Some serial sections were stained with hematoxylin and eosin (Sigma-Aldrich).

Testes from adult mice and ovaries from 10-day-old mice were collected and fixed in 4% paraformaldehyde for in situ hybridizations. They were dehydrated, embedded in paraffin, and then serially sectioned. Five- or 7-μm sections were cut and counterstained with methyl green. These sections were then mounted before observation. For whole-mount in situ hybridizations, embryos were rehydrated and bleached in PBT containing 6% hydrogen peroxide. Whole-mount in situ hybridizations of embryos was performed as previously described (Correia and Conlon, 2001).

Immunohistochemistry

Embryos of FVB mice and adult ovaries were fixed in 4% paraformaldehyde and embedded in paraffin according to standard protocols. Adjacent 6-μm sections were used for comparative analysis. Sections were deparaffinized and rehydrated, and some of them were stained with hematoxylin and eosin. Sections were incubated with a 1:300 dilution of purified anti-Duxbl polyclonal antibodies or with 1:500 dilution of mouse monoclonal anti-MyoD antibody clone 5.8A (IMGENEX). After washing, sections were incubated with a 1:200 dilution of biotinylated goat anti-rabbit IgG or biotinylated goat anti-mouse IgG followed by incubation with horse radish peroxidase-streptavidin complexes. Positive signals were visualized by incubation with diaminobenzidine (DAB), a kit from Molecular Probes, and sections were then lightly counterstained with methyl green (Sigma-Aldrich). Negative controls consisted of identical reactions with normal rabbit immunoglobulin G as the primary antibodies.

Cell Cultures

C2C12 cells were kept in DMEM supplemented with 10% fetal bovine serum. Differentiation in C2C12 cells was induced by replacing the medium with differentiation medium (2% horse serum in DMEM). HeLa cells were kept in alpha-MEM supplemented with 10% fetal calf serum, 1% nonessential amino acids, and 1% sodium pyruvate.

Subcellular Localizations of Duxbl and Duxbl-s Proteins

The coding regions of *Duxbl* and *Duxbl-s* were inserted into pcDNA3.1/V5-His (Life technologies) and pFLAG-CMV2 (Sigma-Aldrich) to produce the Duxbl-V5 and FLAG-Duxbl-s expression vectors, respectively. The expression vectors were transfected into HeLa cells using Lipofectamine 2000 (Invitrogen) according to the manufacturer's instructions. After transfection, cells were immunostained with a 1:500 dilution of purified anti-Duxbl polyclonal antibodies and then a 1:200 dilution of fluorescein isothiocyanate (FITC) -conjugated goat anti-rabbit immunoglobulin. After immunostaining, cell nuclei were counterstained with 4′-6-diamidino-2-phenylindole (DAPI; Sig-ma-Aldrich). The fluorescent signals were obtained by fluorescence microscopy (Axioplan, Zeiss).

Immunocytochemistry

Expressions of Duxbl and MyoD proteins in C2C12 cells were examined by immunocytochemistry. C2C12 myoblasts were grown in 4-well chamber slides and were allowed to differentiate into myotubes. The cells were then fixed in 4% paraformaldehyde followed by permeable with 0.1% Triton. Cells were blocked with 1% bovine serum albumin in phosphate buffered saline (PBS). C2C12 cells were immunostained with rabbit anti-Duxbl (1:500) polyclonal antibodies and mouse monoclonal anti-MyoD (1:500) antibody. Cells were washed with PBS, incubated with FITC-conjugated chicken anti-mouse IgG antibodies and Texas red-conjugated goat anti-rabbit IgG antibodies at a 1:300 dilution, and then counterstained for nuclei with DAPI. The fluorescent signals were obtained by fluorescence microscopy.

ACKNOWLEDGMENTS

We thank Dr. Anita for editing this manuscript.

REFERENCES

Beckers M, Gabriels J, van der Maarel S, De Vriese A, Frants RR, Collen D, Belayew A. 2001. Active genes in junk DNA? Characterization of DUX genes embedded within 3.3 kb repeated elements. Gene 264:51–57.

Belayew A. 2004. Functional study of a gene candidate for Landouzy-Dejerine muscular dystrophy. Bull Mem Acad R Med Belg 159: 343–348; discussion, 348–349.

Boncinelli E. 1997. Homeobox genes and disease. Curr Opin Genet Dev 7:331–337.

Booth HA, Holland PW. 2007. Annotation, nomenclature and evolution of four novel homeobox genes expressed in the human germ line. Gene 387:7–14.

Bopp D, Burri M, Baumgartner S, Frigerio G, Noll M. 1986. Conservation of a large protein domain in the segmentation gene paired and in functionally related genes of Drosophila. Cell 47: 1033–1040.

Bosnakovski D, Xu Z, Gang EJ, Galindo CL, Liu M, Simsek T, Garner HR, Agha-Mohammadi S, Tassin A, Coppee F, Belayew A, Perlingeiro RR, Kyba M. 2008. An isogenetic myoblast expression screen identifies DUX4-mediated FSHD-associated molecular pathologies. EMBO J 27:2766–2779.

Bosnakovski D, Daughters RS, Xu Z, Slack JM, Kyba M. 2009. Biphasic myopathic phenotype of mouse DUX, an ORF conserved FSHD-related repeats. PLoS One 4:e7003.

Buckingham M, Relaix F. 2007. The role of Pax genes in the development of tissues and organs: Pax3 and Pax7 regulate muscle progenitor cell functions. Annu Rev Cell Dev Biol 23:645–673.

Burglin T. 1994. Comprehensive classification of homeobox gene. In: Duboule D, editor. Guidebook to the Homeobox. Oxford, UK: Genes Oxford University Press. p 27–71.

Cillo C, Cantile M, Faiella A, Boncinelli E. 2001. Homeobox genes in normal and malignant cells. J Cell Physiol 188: 161–169.

Clapp J, Mitchell LM, Bolland DJ, Fantes J, Corcoran AE, Scotting PJ, Armour JA, Hewitt JE. 2007. Evolutionary conservation of a coding function for D4Z4, the tandem DNA repeat mutated in facioscapulohumeral muscular dystrophy. Am J Hum Genet 81:264–279.

Correia KM, Conlon RA. 2001. Whole-mount in situ hybridization to mouse embryos. Methods 23:335–338.

Cusella-De Angelis MG, Lyons G, Sonnino C, De Angelis L, Vivarelli E, Farmer K, Wright WE, Molinaro M, Bouche M, Buckingham M, et al. 1992. MyoD, myogenin independent differentiation of primordial myoblasts in mouse somites. J Cell Biol 116:1243–1255.

Ding H, Beckers MC, Plaisance S, Marynen P, Collen D, Belayew A. 1998. Characterization of a double homeodomain protein (DUX1) encoded by a cDNA homologous to 3.3 kb dispersed repeated elements. Hum Mol Genet 7:1681–1694.

Dixit M, Ansseau E, Tassin A, Winokur S, Shi R, Qian H, Sauvage S, Matteotti C, van Acker AM, Leo O, Figlewicz D, Barro M, Laoudj-Chenivesse D, Belayew A, Coppee F, Chen YW. 2007. DUX4, a candidate gene of facioscapulohumeral muscular dystrophy, encodes a transcriptional activator of PITX1. Proc Natl Acad Sci U S A 104:18157–18162.

Gabriels J, Beckers MC, Ding H, De Vriese A, Plaisance S, van der Maarel SM, Padberg GW, Frants RR, Hewitt JE, Collen D, Belayew A. 1999. Nucleotide sequence of the partially deleted D4Z4 locus in a patient with FSHD identifies a putative gene within each 3.3 kb element. Gene 236:25–32.

Galaviz-Hernandez C, Stagg C, de Ridder G, Tanaka TS, Ko MS, Schlessinger D, Nagaraja R. 2003. Plac8 and Plac9, novel placental-enriched genes identified through microarray analysis. Gene 309:81–89.

Galliot B, de Vargas C, Miller D. 1999. Evolution of homeobox genes: Q50 Paired-like genes founded the Paired class. Dev Genes Evol 209:186–197.

Gehring WJ, Qian YQ, Billeter M, Furukubo-Tokunaga K, Schier AF, Resendez-Perez D, Affolter M, Otting G, Wuthrich K. 1994. Homeodomain-DNA recognition. Cell 78:211–223.

Hewitt JE, Lyle R, Clark LN, Valleley EM, Wright TJ, Wijmenga C, van Deutekom JC, Francis F, Sharpe PT, Hofker M, et al. 1994. Analysis of the tandem repeat locus D4Z4 associated with facioscapulohumeral muscular dystrophy. Hum Mol Genet 3:1287–1295.

Holland PW, Takahashi T. 2005. The evolution of homeobox genes: implications for the study of brain development. Brain Res Bull 66:484–490.

Holland PW, Booth HA, Bruford EA. 2007. Classification and nomenclature of all human homeobox genes. BMC Biol 5:47.

Kablar B, Krastel K, Ying C, Asakura A, Tapscott SJ, Rudnicki MA. 1997. MyoD and Myf-5 differentially regulate the development of limb versus trunk skeletal muscle. Development 124:4729–4738.

Kawazu M, Yamamoto G, Yoshimi M, Yamamoto K, Asai T, Ichikawa M, Seo S, Nakagawa M, Chiba S, Kurokawa M, Ogawa S. 2007. Expression profiling of immature thymocytes revealed a novel homeobox gene that regulates double-negative thymocyte development. J Immunol 179:5335–5345.

Kowaljow V, Marcowycz A, Ansseau E, Conde CB, Sauvage S, Matteotti C, Arias C, Corona ED, Nunez NG, Leo O, Wattiez R, Figlewicz D, Laoudj-Chenivesse D, Belayew A, Coppee F, Rosa AL. 2007. The DUX4 gene at the FSHD1A locus encodes a pro-apoptotic protein. Neuromuscul Disord 17:611–623.

Kozak M. 1996. Interpreting cDNA sequences: some insights from studies on translation. Mamm Genome 7:563–574.

Kozmik Z. 2005. Pax genes in eye development and evolution. Curr Opin Genet Dev 15:430–438.

Li H, Tsai MS, Chen CY, Lian WC, Chiu YT, Chen GD, Wang SH. 2006. A novel maternally transcribed homeobox gene, Eso-1, is preferentially expressed in oocytes and regulated by cytoplasmic polyadenylation. Mol Reprod Dev 73: 825–833.

Mathers PH, Grinberg A, Mahon KA, Jamrich M. 1997. The Rx homeobox gene is essential for vertebrate eye development. Nature 387:603–607.

McGinnis W, Krumlauf R. 1992. Homeobox genes and axial patterning. Cell 68: 283–302.

Miura H, Yanazawa M, Kato K, Kitamura K. 1997. Expression of a novel aristaless related homeobox gene 'Arx' in the vertebrate telencephalon, diencephalon and floor plate. Mech Dev 65:99–109.

Ohtoshi A, Justice MJ, Behringer RR. 2001. Isolation and characterization of Vsx1, a novel mouse CVC paired-like homeobox gene expressed during embryogenesis and in the retina. Biochem Biophys Res Commun 286: 133–140.

Olaso R, Habert R. 2000. Genetic and cellular analysis of male germ cell development. J Androl 21:497–511.

Ostlund C, Garcia-Carrasquillo RM, Belayew A, Worman HJ. 2005. Intracellular trafficking and dynamics of double homeodomain proteins. Biochemistry 44:2378–2384.

Paillisson A, Dade S, Callebaut I, Bontoux M, Dalbies-Tran R, Vaiman D, Monget P. 2005. Identification, characterization and metagenome analysis of oocyte-specific genes organized in clusters in the mouse genome. BMC Genomics 6:76.

Pang AL, Taylor HC, Johnson W, Alexander S, Chen Y, Su YA, Li X, Ravindranath N, Dym M, Rennert OM, Chan WY. 2003. Identification of differentially expressed genes in mouse spermatogenesis. J Androl 24:899–911.

Ploski JE, Shamsher MK, Radu A. 2004. Paired-type homeodomain transcription factors are imported into the nucleus by karyopherin 13. Mol Cell Biol 24: 4824–4834.

Ramos CR, Abreu PA, Nascimento AL, Ho PL. 2004. A high-copy T7 Escherichia coli expression vector for the production of recombinant proteins with a minimal N-terminal His-tagged fusion peptide. Braz J Med Biol Res 37:1103–1109.

Sassoon D, Lyons G, Wright WE, Lin V, Lassar A, Weintraub H, Buckingham M. 1989. Expression of two myogenic regulatory factors myogenin and MyoD1 during mouse embryogenesis. Nature 341:303–307.

Tajbakhsh S, Buckingham M. 2000. The birth of muscle progenitor cells in the mouse: spatiotemporal considerations. Curr Top Dev Biol 48:225–268.

Tupler R, Gabellini D. 2004. Molecular basis of facioscapulohumeral muscular dystrophy. Cell Mol Life Sci 61:557–566.

van Deutekom JC, Wijmenga C, van Tienhoven EA, Gruter AM, Hewitt JE, Padberg GW, van Ommen GJ, Hofker MH, Frants RR. 1993. FSHD associated DNA rearrangements are due to deletions of integral copies of a 3.2 kb tandemly repeated unit. Hum Mol Genet 2: 2037–2042.

Wang SH, Tsai MS, Chiang MF, Li H. 2003. A novel NK-type homeobox gene, ENK (early embryo specific NK), preferentially expressed in embryonic stem cells. Gene Expr Patterns 3:99– 103.

Wijmenga C, Hewitt JE, Sandkuijl LA, Clark LN, Wright TJ, Dauwerse HG, Gruter AM, Hofker MH, Moerer P, Williamson R, et al. 1992. Chromosome 4q DNA rearrangements associated with facioscapulohumeral muscular dystrophy. Nat Genet 2:26–30.

Winokur ST, Bengtsson U, Feddersen J, Mathews KD, Weiffenbach B, Bailey H, Markovich RP, Murray JC, Wasmuth JJ, Altherr MR, et al. 1994. The DNA rearrangement associated with facioscapulohumeral muscular dystrophy involves a heterochromatin-associated repetitive element: implications for a role of chromatin structure in the pathogenesis of the disease. Chromosome Res 2:225–234.

國科會補助計畫衍生研發成果推廣資料表

日期:2011/10/31

國科會補助計畫	計畫名稱: 小鼠染色體14A3區性腺表現基因群的分子特性與功能分析
	計畫主持人: 王淑紅
	計畫編號: 97-2320-B-040-010-MY3　　學門領域: 醫學之生化及分子生物

無研發成果推廣資料

97 年度專題研究計畫研究成果彙整表

計畫主持人：王淑紅	計畫編號：97-2320-B-040-010-MY3
計畫名稱：小鼠染色體 14A3 區性腺表現基因群的分子特性與功能分析	

成果項目			量化			單位	備註（質化說明：如數個計畫共同成果、成果列為該期刊之封面故事...等）
			實際已達成數（被接受或已發表）	預期總達成數(含實際已達成數)	本計畫實際貢獻百分比		
國內	論文著作	期刊論文	0	0	100%	篇	
		研究報告/技術報告	0	0	100%		
		研討會論文	10	10	100%		
		專書	0	0	100%		
	專利	申請中件數	0	0	100%	件	
		已獲得件數	0	0	100%		
	技術移轉	件數	0	0	100%	件	
		權利金	0	0	100%	千元	
	參與計畫人力（本國籍）	碩士生	2	0	100%	人次	
		博士生	0	0	100%		
		博士後研究員	0	0	100%		
		專任助理	0	0	100%		
國外	論文著作	期刊論文	1	3	100%	篇	
		研究報告/技術報告	0	0	100%		
		研討會論文	0	0	100%		
		專書	0	0	100%	章/本	
	專利	申請中件數	0	0	100%	件	
		已獲得件數	0	0	100%		
	技術移轉	件數	0	0	100%	件	
		權利金	0	0	100%	千元	
	參與計畫人力（外國籍）	碩士生	0	0	100%	人次	
		博士生	0	0	100%		
		博士後研究員	0	0	100%		
		專任助理	0	0	100%		

其他成果 (無法以量化表達之成果如辦理學術活動、獲得獎項、重要國際合作、研究成果國際影響力及其他協助產業技術發展之具體效益事項等，請以文字敘述填列。)	無

	成果項目	量化	名稱或內容性質簡述
科教處計畫加填項目	測驗工具(含質性與量性)	0	
	課程/模組	0	
	電腦及網路系統或工具	0	
	教材	0	
	舉辦之活動/競賽	0	
	研討會/工作坊	0	
	電子報、網站	0	
	計畫成果推廣之參與（閱聽）人數	0	

國科會補助專題研究計畫成果報告自評表

請就研究內容與原計畫相符程度、達成預期目標情況、研究成果之學術或應用價值（簡要敘述成果所代表之意義、價值、影響或進一步發展之可能性）、是否適合在學術期刊發表或申請專利、主要發現或其他有關價值等，作一綜合評估。

1. 請就研究內容與原計畫相符程度、達成預期目標情況作一綜合評估

■達成目標

□未達成目標（請說明，以 100 字為限）

□實驗失敗

□因故實驗中斷

□其他原因

說明：

2. 研究成果在學術期刊發表或申請專利等情形：

論文：■已發表 □未發表之文稿 □撰寫中 □無

專利：□已獲得 □申請中 ■無

技轉：□已技轉 □洽談中 ■無

其他：(以 100 字為限)

目前有兩篇報告撰寫中

3. 請依學術成就、技術創新、社會影響等方面，評估研究成果之學術或應用價值（簡要敘述成果所代表之意義、價值、影響或進一步發展之可能性）(以 500 字為限）

本研究發現兩個新穎生殖細胞專一性表達基因 Cphx 及 Gcse,及一個人類 FSHD 疾病致病基因 DUX4 之同源基因 Duxbl,其中 Cphx 以 RNAi 技術分別以基因轉殖及體外 microinjection 的方式降低 Cphx 基因的表現,研究發現 Cphx-dsRNA 轉殖鼠生殖能力降低,同時提早不孕,而 microinjection Cphx dsRNA 也影響卵細胞的成熟與早期胚胎發育，我們推測 Cphx 基因影響卵細胞成熟發育及早期胚胎之發育， Cphx 基因之研究，在學術上可以幫助我們了解複雜的生殖細胞發育機制,在社會影響方面同時也可以幫助我們解開人類不孕症與卵巢提早老化之謎，將來進一步找出人類 CPHX 基因，同時分析不孕症病人或卵巢提早老化病人其 CPHX 基因是否異常，將有助我們了解不孕症之成因。另外一個生殖細胞專一性表達基因 Gcse，根據我們的結果顯示，與生殖細胞減數分裂及 acrosome 的形成有關，減數分裂正常與否將影響單倍體生殖細胞之合成，而 acrosome 是受精作用必要的胞器，是決定精細胞與卵細胞結合之重要構造，因此，對 Gcse 基因的研究將有助於我們對單倍體生殖細胞之產生與受精作用的了解,對於不孕症病人生殖細胞數目為何異常及為何精細胞無法與卵細胞結合有更進一步的了解，最後一個基因 Duxbl 雖然也表現於生殖細胞，但也表現於骨骼肌，更重要的是人類 FSHD 疾病致病基因 DUX4 之同源基因，對 Duxbl 的研究將有助於我們了解骨骼肌發育及 FSHD 之致病機制，進而找到 FSHD 治療的方法，目前我們的研究顯示 Duxbl 基因異常的表現將抑制肌纖維的分化,無法形成多核的肌小管,根據我們 Duxbl 基因之研究成果，將來可以建立 FSHD 疾病的小鼠模式，將可以協助我們進一步了解 FSHD

致病機制及找出治療 FSHD 疾病的方法。